# A Model of Decadal Middle-Latitude Atmosphere–Ocean Coupled Modes

JASON GOODMAN AND JOHN MARSHALL

*Program in Atmospheres, Oceans and Climate, Department of Earth, Atmospheric and Planetary Sciences, Massachusetts Institute of Technology, Cambridge, Massachusetts*

(Manuscript received 7 July 1997, in final form 9 March 1998)

ABSTRACT

An analytical model of the mutual interaction of the middle-latitude atmosphere and ocean is formulated and studied. The model is found to support coupled modes in which oceanic baroclinic Rossby waves of decadal period grow through positive coupled feedback between the thermal forcing of the atmosphere induced by SST anomalies and the resulting wind stress forcing of the ocean. Growth only occurs if the atmospheric response to thermal forcing is equivalent barotropic, with a particular phase relationship with the underlying SST anomalies. The dependence of the growth rate and structure of the modes on the nature of the assumed physics of air–sea interaction is explored, and their possible relation to observed phenomena discussed.

## 1. Introduction

There is a growing body of literature that documents the existence of covarying patterns of oceanic and atmospheric climate variability on decadal timescales. For example, Hurrell (1995) and Kushnir (1994) discuss atmospheric variability patterns, Dickson et al. (1996), McCartney et al. (1997), and Curry and McCartney (1997) consider oceanic changes, and Cayan (1992a,b), Deser and Blackmon (1993), and Sutton and Allen (1997) describe patterns covariant between atmosphere and ocean. But the underlying dynamical causes of this variability remain obscure. We do not yet know whether the dynamics are coupled or uncoupled, nor do we know the relative importance of the ocean and atmosphere on decadal timescales. Does variability arise through internal instabilities in one component only, which communicates these changes to its passive partner, or does it arise through mutual interactions of the two systems? Useful review of these issues is given by Palmer (1996) and McCartney et al. (1997). Frankignoul (1985) concisely reviews middle-latitude atmosphere–ocean interactions.

Many researchers suggest the atmosphere generates the climate variations on its own, and the ocean reacts passively to that stimulus. Some modeling studies (e.g., James and James 1989) show that a model atmosphere is capable, in the presence of fixed surface boundary conditions (fixed ocean), of exhibiting long-term persistent (climate) states, in clear contradiction to the usual assertion that the atmosphere has no memory longer than about one month. Such persistence in small regions of phase space is a manifestation of Lorenz's (1975) description of the atmosphere as nearly intransitive. Atmospheric general circulation models, forced with temporally nonvarying SSTs, display fluctuations that resemble the spatial structure of observed modes of variability such as the North Atlantic Oscillation [NAO; Barnett 1985; Marshall and Molteni 1993] but do not capture the reddening of observed spectra.

The idea that much of observed climate variability can be explained as the integral response of the slowly varying parts of the climate system to stochastic atmospheric variability was first proposed by Hasselmann (1976) and Frankignoul and Hasselmann (1977); see also Cayan (1992a,b), Battisti et al. (1995) and Hall and Manabe (1997). Frankignoul et al. (1997) have shown that decadal timescales in a dynamical ocean can be generated through the response of oceanic baroclinic Rossby waves to stochastic wind stress forcing. Griffies and Tziperman (1995) attribute decadal fluctuations of the thermohaline circulation evident in coupled integrations to stochastic atmospheric forcing. But the purely stochastic model is inconsistent with the observed, albeit rather slight, reddening of atmospheric spectra (see, e.g., Deser and Blackmon 1993).

One possible mechanism that could account for a reddened atmospheric spectrum is that the ocean ''imprints'' itself back on the atmosphere on longer timescales. It could do this by inducing a response from (on these long timescales) a passive atmosphere or through an active dynamical coupling with the atmosphere. We find it useful to call the former process ''passive cou-

*Corresponding author address:* Mr. Jason Goodman, Department of Earth, Atmospheric & Planetary Sciences, MIT, Room 54-1515, Cambridge, MA 02139.
E-mail: goodmanj@mit.edu

pling'' and the latter ''active coupling.'' Passive coupling is a feature of the models studied by Saravanan and McWilliams (1997, 1998) and Weng and Neelin (1998). An example of active coupling in a coupled atmosphere–ocean numerical model is described in Latif and Barnett (1996) and Latif et al. (1996).

In this paper we construct an analytical model of active coupling and study how a dynamical ocean in middle and high latitudes might actively couple to the atmosphere. We formulate and analyze a simple coupled atmosphere–ocean model in which SST depends on ocean dynamics modulated by wind-stress-curl forcing as well as air–sea interaction. Growing modes of decadal period are found and we study their form and dependence on the coupling physics assumed.

In section 2 the coupled model is formulated. In section 3, the dispersion relation and structure of the coupled modes is derived. In section 4, we discuss these solutions in the context of observations of observed phenomena such as the Antarctic Circumpolar Wave and the North Atlantic Oscillation, and their parameter sensitivity. Conclusions are presented in section 5.

## 2. Model formulation

### a. Overview

Our model comprises a quasi-geostrophic atmosphere overlying a quasigeostrophic ocean, characterized by their respective potential vorticities (QGPV) and streamfunction distributions and governed by prognostic QGPV equations on a beta plane.

The atmosphere, imagined to be bounded above by a lid and below by the ocean, is governed by the equation

$$\frac{D}{Dt}q_a = f_o\frac{\partial}{\partial z}\left(\frac{Q_a}{\dfrac{\partial}{\partial z}\overline{\theta_a}}\right) - \epsilon\nabla^2\psi_{as} \quad \text{(atmosphere)}. \quad (1)$$

Here $D/Dt$ is the Lagrangian derivative and $q_a$ is the quasigeostrophic potential vorticity,

$$q_a = \nabla^2\psi_a + \beta y + f_o^2\frac{\partial}{\partial z}\left(\frac{1}{N_a^2}\frac{\partial}{\partial z}\psi_a\right),$$

expressed in terms of the atmospheric streamfunction $\psi_a$. Here, $f_o$ is a reference value of the Coriolis parameter $f$, the meridional gradient of $f$ is $\beta$, $N_a^2 = (1/\theta_{a0})(\partial/\partial z)\overline{\theta_a}$ is the atmospheric Brunt–Väisälä buoyancy frequency, $\theta_a$ the atmospheric potential temperature with $\theta_{a0}$ a typical value, and $Q_a$ is the diabatic heating rate of the atmosphere defined by

$$\frac{D}{Dt}\theta_a = Q_a. \quad (2)$$

In (1), $\epsilon\nabla^2\psi_{as}$ represents frictional sinks of vorticity associated with Ekman layers at the surface with $\epsilon^{-1}$ a frictional spindown time.

We suppose that a radiative-convective equilibrium temperature, $\theta_a^*$, controls the thermal forcing of the atmosphere thus

$$Q_a = -\gamma_a(\theta_a - \theta_a^*). \quad (3)$$

Here $\gamma_a^{-1}$ is a timescale set by the radiative-convective process; the value $\theta_a^*$ is a radiative-convective temperature profile to which $\theta_a$ relaxes, which is assumed to be a function of sea surface temperature thus

$$\theta_a^* = \theta_a^*(\text{SST}). \quad (4)$$

The form, (3) and (4), makes sense as a simple and physically plausible representation of convective heating of the troposphere, permitting the heating field to be a function of the state of both the atmosphere and the ocean. That heating will initiate a dynamical response of the atmosphere and change the winds that blow over the ocean.

The equations governing the ocean are

$$\frac{D}{Dt}q_o = f_o\frac{\partial}{\partial z}\left(\frac{Q_o}{\dfrac{\partial}{\partial z}\overline{\theta_o}}\right) + \frac{1}{\rho_o}\hat{k}\cdot\boldsymbol{\nabla}\times\frac{\partial}{\partial z}\boldsymbol{\tau} \quad \text{(ocean)}, \quad (5)$$

where $q_o$ is the oceanic QGPV,

$$q_o = \nabla^2\psi_o + \beta y + f_o^2\frac{\partial}{\partial z}\left(\frac{1}{N_o^2}\frac{\partial}{\partial z}\psi_o\right),$$

$\psi_o$ is an oceanic streamfunction, $N_o^2$ is an oceanic Brunt–Väisälä frequency, $Q_o$ is the diabatic heating of the interior of the ocean, and $\boldsymbol{\tau}$ is the mechanical stress supplied by the surface wind. The stress at the ocean's surface is a function of the velocity of the wind at the surface

$$\boldsymbol{\tau}_s = \boldsymbol{\tau}_s(\psi_s). \quad (6)$$

The evolution of the oceanic mixed layer temperature, which we assume is synonymous with sea surface temperature, is

$$\left(\frac{\partial}{\partial t} + \boldsymbol{\upsilon}\cdot\boldsymbol{\nabla}\right)\text{SST} = Q_o \quad \text{(sea surface temperature)}. \quad (7)$$

Here the horizontal velocity in the mixed layer is $\boldsymbol{\upsilon}$, the sum of an Ekman and geostrophic components ($\boldsymbol{\upsilon} = \boldsymbol{\upsilon}_{ek} + \boldsymbol{\upsilon}_g$), and $Q_o$ is the diabatic heating of the mixed layer induced by air–sea interaction and entrainment fluxes through the mixed layer base. There is no vertical advection in Eq. (7) because the mixed layer is assumed to be vertically homogeneous.

Note the following.

1) Equations (1) and (2) are the starting point of analytical studies of atmospheric planetary waves dating back to Charney and Eliassen (1949) and Smagorinsky (1953).
2) If $\boldsymbol{\upsilon} = w = 0$, then (7) reduces to a ''slab ocean,''

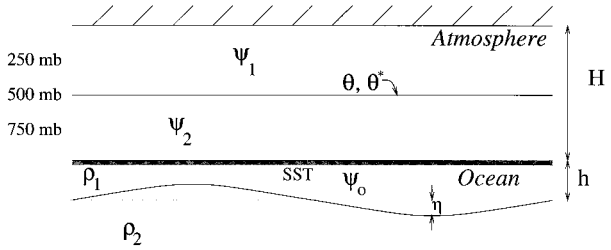


FIG. 1. Vertical structure of the coupled model defining the key variables of the coupled ocean–atmosphere system.

which responds on timescales of several months (primarily via surface heat exchange and entrainment), depending on the depth of the slab [see, e.g., Hasselman (1976); Frankignoul and Hasselman (1977)]. On decadal timescales, however, advective processes may be important and SST changes may be dominated by gyre dynamics and subduction processes ($v$ and $w$): see Hall and Manabe (1997).

3) If the wind-curl is assumed to be a stochastic process and $Q_o = 0$ in Eq. (5), then it reduces to the ocean model analyzed by Frankignoul et al. (1997) in their study of the response of the ocean to stochastic atmospheric forcing.

Clearly, (1)–(7) are highly simplified representations of the respective fluids and their interaction. But the philosophy of our approach is to build our intuition about the coupled problem in stages, by first fitting together simple pieces, and then increasing the complexity of the component parts and their coupling. Heating of the atmosphere depends, through (3) and (4), on the state of the ocean which, in turn, depends on its forcing from the atmosphere via (6). We shall now go on to study whether the above system supports coupled modes. Their existence will depend on the form assumed for (3), (4), (6), and (7), that is, on the nature of the boundary layers of the two fluids and the manner in which they are assumed to interact with one another and the ''free'' atmosphere/ocean above/below. To make analytical progress our representations will, of necessity, be simple, but they are motivated by sound physical principles.

### *b. Atmosphere*

We will adopt the simplest representation of the equation set described in section 2a, which captures the essential dynamics; a two-level quasigeostrophic atmosphere, sketched schematically in Fig. 1. This model is extremely simple and limited in scope (particularly in its ability to resolve the vertical structure of atmospheric heating) but it has been comprehensively studied and allows us to obtain analytical solutions. Furthermore it is supposed that the atmosphere responds rapidly to thermal forcing associated with SST anomalies when compared to interannual-to-decadal timescales, and so on these timescales the atmosphere is assumed to be in steady state. We therefore neglect the local time-derivative terms in the prognostic equations for the atmosphere, thus slaving it to SST. No attempt is made to represent the rectified affects of high-frequency components on the steady circulation (the interaction of synoptic eddies with the planetary-wave pattern, for example). We recognize that this is an important process in nature, but one which is difficult to address in a simple model.

For simplicity we also set $\epsilon = 0$ in (1), thus obtaining the following the two-level, steady-state quasigeostrophic equations for the atmosphere [using the nomenclature of Shutts (1987)],

$$J(\psi_2, q_2) = \frac{gHS}{2fL_a^2}; \qquad J(\psi_1, q_1) = -\frac{gHS}{2fL_a^2},$$

where $S$ is the diabatic forcing, given by $S = Q_a/\theta_{a0}$, $\theta_{a0}$ is a typical atmospheric temperature, and

$$q_1 = \nabla^2\psi_1 - \frac{1}{L_a^2}(\psi_1 - \psi_2) + \beta y$$

$$q_2 = \nabla^2\psi_2 + \frac{1}{L_a^2}(\psi_1 - \psi_2) + \beta y$$

are the QGPVs at each level with $L_a^2 = (N_a^2H^2)/(4f^2)$ the square of the atmospheric baroclinic Rossby radius.

Taking the sum and difference of $\psi$ and $q$ to form the barotropic and baroclinic streamfunction and PV, and using the notation $\hat{a} = a_2 + a_1$; $\tilde{a} = a_1 + a_2$, equations for the barotropic and baroclinic PV can be written thus

$$J(\hat{\psi}, \hat{q}) + J(\tilde{\psi}, \tilde{q}) = 0 \quad \text{(barotropic)} \quad \text{and} \quad (8)$$

$$J(\tilde{\psi}, \hat{q}) + J(\hat{\psi}, \tilde{q}) = -\frac{2gHS}{fL_a^2} \quad \text{(baroclinic)}, \quad (9)$$

where

$$\hat{q} = q_2 + q_1 = \nabla^2\hat{\psi} + 2\beta y$$

$$\tilde{q} = q_1 - q_2 = \nabla^2\tilde{\psi} - \frac{2}{L_a^2}\tilde{\psi}.$$

Planetary $\beta$ appears only in the barotropic PV; the stretching term appears only in the baroclinic PV.

It should be noted that diabatic heating only directly forces the baroclinic PV equation. However, because the baroclinic fields drive the barotropic PV equation through (8), the atmosphere does not respond purely baroclinically. Thermal forcing can yield an ''equivalent barotropic'' response (anomalies of constant sign throughout the atmosphere) and need not always result in first-baroclinic mode behavior. This turns out to be crucial to the existence of coupled modes in our simple model (see section 3).

### 1) Linearized model

We linearize the atmospheric equations around the simplest realistic state: uniform zonal winds of differing magnitudes at levels 1 and 2. Again, defining barotropic and baroclinic components, $\hat{U} = U_1 + U_2$; $\tilde{U} = U_1 - U_2$, we have

$$\hat{\psi} = \hat{\psi}' - \hat{U}y \qquad \tilde{\psi} = \tilde{\psi}' - \tilde{U}y.$$

Substituting into (8) and (9) and neglecting quadratic terms in the perturbation quantitites, we have (after dropping the primes to simplify notation) the barotropic PV equation

$$\hat{U}\frac{\partial}{\partial x}(\nabla^2\hat{\psi} + \hat{\beta}y) + \hat{\beta}\frac{\partial}{\partial x}\hat{\psi} + \tilde{U}\frac{\partial}{\partial x}(\nabla^2\tilde{\psi} + \tilde{\beta}y) = 0, \tag{10}$$

and the baroclinic PV equation

$$\tilde{U}\frac{\partial}{\partial x}(\nabla^2\hat{\psi} + \hat{\beta}y) + \tilde{\beta}\frac{\partial}{\partial x}\hat{\psi} + \hat{U}\frac{\partial}{\partial x}\left(\nabla^2\tilde{\psi} - \frac{2}{L_a^2}\tilde{\psi} + \tilde{\beta}y\right) + \hat{\beta}\frac{\partial}{\partial x}\tilde{\psi} = -\frac{2gHS}{fL_a^2}, \tag{11}$$

where

$$\hat{\beta} = 2\beta \tag{12}$$

enters as a beta-effect term in the barotropic PV[1] and

$$\tilde{\beta} = \frac{2}{L_a^2}\tilde{U} \tag{13}$$

plays the same role in the baroclinic PV. Note how two different mechanisms provide the same effect: The $\hat{\beta}$ arises from changes in planetary vorticity; $\tilde{\beta}$ arises from vortex-stretching when fluid moves against the sloping interface generated by the zonal mean wind shear $\tilde{U}$.

Following Shutts (1987), we specify a Newtonian relaxation of the temperature perturbation (at level 1½) toward some equilibrium temperature anomaly $\delta\phi^*$ [$\phi = \ln\theta$; $\delta\phi = (\delta\theta)/(\theta_{a0})$] on a radiative-convective equilibrium timescale $1/\gamma_a$

$$S = -\gamma_a(\delta\phi - \delta\phi^*) = -\gamma_a\left(\frac{2f}{gH}\tilde{\psi} - \frac{\theta_a^*}{\theta_{a0}}\right), \tag{14}$$

where we have expressed the temperature in the quasigeostrophic model in terms of the baroclinic streamfunction by using $\delta\phi = (2f)/(gH)\tilde{\psi}$, employing the thermal wind relation.

Inserting (14) into (11), we have

$$\tilde{U}\frac{\partial}{\partial x}(\nabla^2\hat{\psi} + \hat{\beta}y) + \tilde{\beta}\frac{\partial}{\partial x}\hat{\psi} + \hat{U}\frac{\partial}{\partial x}\left(\nabla^2\tilde{\psi} - \frac{2}{L_a^2}\tilde{\psi} + \tilde{\beta}y\right) + \hat{\beta}\frac{\partial}{\partial x}\tilde{\psi} = \frac{4\gamma_a}{L_a^2}\left(\tilde{\psi} - \frac{1}{r_a}\theta_a^*\right), \tag{15}$$

where

$$r_a \equiv \frac{2f\theta_{a0}}{gH}$$

has units of (temperature/streamfunction), and converts atmospheric temperature to baroclinic streamfunction through the thermal wind relation. Thus thermal forcing of the atmosphere drives it toward an equilibration streamfunction $\tilde{\psi}^* = \theta_a^*/r_a$.

### 2) Thermally forced and equilibrated responses

The properties of the above system for a specified $\theta_a^*$ are described in detail by Shutts (1987) and Marshall and So (1990); see also Frankignoul (1985). Because of the form chosen for the forcing function (14), the driving of the atmosphere by diabatic heating depends on the response of the atmosphere to that heating. In more conventional forcing problems, $S$ is prescribed as a fixed and unchanging function of space. Then the thermal response of the atmosphere is always 90° out of phase with the heating field [note the odd number of derivatives on the left side of (15), so that if $S$ varies sinusoidally the response will vary cosinusoidally], either upstream or downstream depending on the strength of the wind relative to the free Rossby wave speed. Indeed in Fig. 2a, in which the zonal winds are chosen to be considerably stronger than the free Rossby wave speed, we see lows at the surface, downstream of the warming and the vertical structure of the atmospheric response is baroclinic, with highs above lows and vice-versa. This is the classical picture of direct thermal forcing of the atmosphere. However, Shutts (1987) shows that ''equilibration'' can occur at the scale of free, stationary Rossby waves if the forcing is assumed to be a function of the atmosphere's response as in (3). At equilibration the left and right sides of (15) vanish independently. In this case (see Fig. 2b), on a scale close to that at which Rossby waves are stationary with respect to the ground, the response is equivalent barotropic, with highs directly over warm $\theta_a^*$ and lows over cold $\theta_a^*$. At this resonance scale, the response of the atmosphere is not infinite, however. Rather the diabatic heating rates become vanishingly small (equilibration occurs) as $\theta_a \rightarrow \theta_a^*$.

[1] The factor of 2 arises because we have defined the barotropic fields as vertical sums rather than averages.

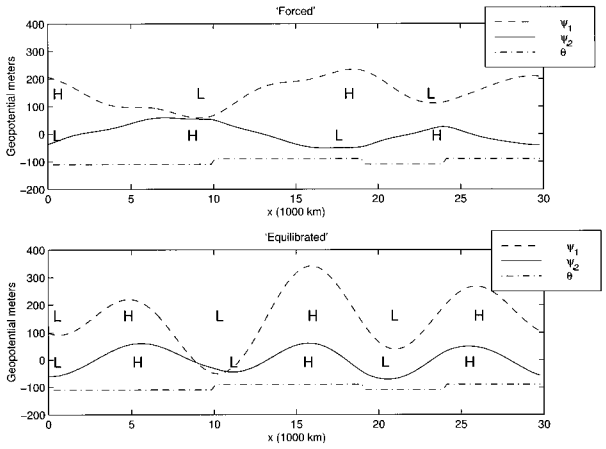


FIG. 2. Steady-state atmospheric response to thermal forcing [reproduced from Shutts (1987)]. Dashed curves: upper-level height anomaly, offset 150 gpm. Solid curves: lower-level height anomaly. Dash–dotted curve: equilibration temperature anomaly $\theta_a^*$, (amplitude 10°C). Shutts' $\theta_a^*$ profile is chosen to broadly represent land–ocean differences in the wintertime Northern Hemisphere: $\theta_a^*$ is higher over oceans than land. (a) Directly forced response of atmospheric model to thermal forcing, with ($U_1 = 10$ m s$^{-1}$, $U_2 = 5$ m s$^{-1}$). For the dominant wavenumber 3, $\mu = +\frac{1}{3}$ from (31) and $\nu/\Gamma = 2.7$, from (32) and (33): the response is baroclinic and strongly phase-shifted. (b) Equilibrated response, with ($U_1 = 20$ m s$^{-1}$, $U_2 = 7$ m s$^{-1}$). For wavenumber 3, $\mu = -3$, $\nu/\Gamma = 0.5$. Response is barotropic with ridges over warm $\theta_a^*$ and troughs over cold $\theta_a^*$; the phase shift is small.

### c. Ocean

We adopt quasigeostrophic dynamics in a ''1½-layer'' ocean, with a moving upper layer and a very deep lower layer that remains at rest; there is a a rigid lid at the surface (Pedlosky 1987). Neglecting thermal PV sources [$Q_o = 0$ in (5)], the potential vorticity in the upper layer of ocean evolves according to (see Fig. 1)

$$\frac{D}{Dt}q_o = \nabla \times \frac{\tau}{\rho_{o0}h},$$

where

$$q_o = \nabla^2\psi_o - \frac{1}{L_o^2}\psi_o + \beta y.$$

Here $\psi_o$ is the oceanic streamfunction in the upper layer, $L_o^2 \equiv (gh\Delta\rho/\rho_{o0})/f^2$ is the square of the oceanic baroclinic Rossby radius of deformation, with $\rho_{o0}$ a constant reference value of density and $\Delta\rho$ the density difference between the two layers. Linearizing about a state of rest we have

$$\frac{\partial}{\partial t}\left(\nabla^2\psi_o - \frac{1}{L_o^2}\psi_o\right) + \beta\frac{\partial}{\partial x}\psi_o = \frac{1}{\rho_{o0}}\nabla \times \frac{\tau}{h}.$$

We are interested in motions with spatial extents ($L$) of thousands of km. The Rossby radius in the ocean ($L_o$) is ~50 km, so we may make the longwave approximation and neglect the relative vorticity contribution to the PV, giving our final equation for the dynamic ocean

$$-\frac{1}{L_o^2}\frac{\partial}{\partial t}\psi_o + \beta\frac{\partial}{\partial x}\psi_o = \frac{1}{\rho_{o0}}\nabla \times \frac{\tau}{h}. \tag{16}$$

### d. Coupling mechanisms

#### 1) WIND STRESS

With our simplified representations of atmosphere and ocean defined, we now specify the mutual forcing between them. The model ocean's circulation is forced by the stress generated by the surface wind field. We suppose that the wind stress perturbation is proportional to the surface wind velocity perturbation, and set

$$\frac{1}{\rho_{o0}}\nabla \times \frac{\tau}{h} = \alpha\nabla^2\psi_s. \tag{17}$$

Here, $\psi_s = \psi_2 + 1(\psi_2 - \psi_1)/2 = (\hat{\psi} - \tilde{\psi})/2$ is the atmospheric streamfunction extrapolated to the surface. The numerical values of the constant of proportionality, $\alpha$, which depends on the air–sea drag coefficient, will be considered in section 4b.

#### 2) THERMAL FORCING

As in (4), we suppose that the atmosphere equilibrates to a temperature set by the sea surface. For simplicity, we set the equilibration temperature anomaly equal to SST′,

$$\theta_a^* = \mathrm{SST}'. \tag{18}$$

How shall we determine the sea surface temperature? Following Frankignoul (1985), we begin with the following equation for the evolution of mixed layer temperature anomalies (assumed synonymous with SST):

$$h_{\mathrm{mix}}\frac{\partial}{\partial t}\mathrm{SST}' = -\frac{\lambda_o}{\rho C_p}(\mathrm{SST}' - \theta_a') - h_{\mathrm{mix}}\mathbf{u}' \cdot \nabla\overline{\mathrm{SST}} - w_e(\mathrm{SST}' - \theta_{\mathrm{sub}}), \tag{19}$$

where $h_{\mathrm{mix}}$ is the mixed layer depth, SST′ is the sea surface temperature anomaly, $\theta_a'$ is the surface air temperature, $\lambda_o$ is the linearized coefficient of combined latent, sensible, and longwave heat flux, $u'$ is the anomaly in current in the mixed layer, $\nabla\overline{\mathrm{SST}}$ is the mean SST gradient, $w_e$ is the entrainment velocity at the base of the mixed layer, and $\theta_{\mathrm{sub}}$ is the temperature of the thermal anomaly being entrained.

If the $\theta_a'$ induced by the SST anomaly does not exceed the SST anomaly itself (a reasonable assumption on interannual and longer timescales) then the terms in our SST equation have the following magnitudes:

$$\sigma \sim \frac{\lambda_o}{C_o} + U\frac{\nabla\overline{\mathrm{SST}}}{\mathrm{SST}'} + \frac{w_e}{h_{\mathrm{mix}}},$$

where $\sigma$ is the frequency at which SST is changing, $C_o$

$= \rho c_p h_{\text{mix}}$ is the heat capacity of the mixed layer of depth $h_{\text{mix}}$, and $U$ is a measure of the strength of the current anomaly.

On interannual/decadal timescales $\sigma \sim 2\pi/(10\text{ yr}) \sim 2 \times 10^{-8}\text{ s}^{-1}$. Estimates of the atmospheric heat flux feedback, $\lambda_o$, are given in Frankignoul et al. (1997) and Barsugli and Battisti (1998) and suggest a value of $\lambda_o \sim 20\text{ W m}^{-2}\text{ K}^{-1}$. The heat capacity of a mixed layer of depth 100 m is $C_o \sim 4 \times 10^8\text{ J m}^{-2}\text{ K}^{-1}$ and so $\lambda_o/C_o \sim 5 \times 10^{-8}\text{ s}^{-1}$, of the same order as $\sigma$. In the advection term, a circulation anomaly associated with a 1° SST anomaly might be 2 cm s$^{-1}$, so given a 10°C (3000 km)$^{-1}$ mean meridional SST gradient, the advection term is $\sim 7 \times 10^{-8}\text{ s}^{-1}$. Finally, consider the entrainment term. During the summer $w_e$ is close to zero, but $w_e$ is large during the rapid deepening of the mixed layer in the winter. If the mixed layer deepens to 200 m during the six winter months (its thickness $h$ averaging 100 m over this period) then $w_e/h_{\text{mix}} \sim (1/100)(200/0.5\text{ yr}) = 1.3 \times 10^{-7}\text{ s}^{-1}$. The observed annual mean is roughly $7 \times 10^{-8}\text{ s}^{-1}$ over most of the midlatitude oceans, being zero during summer restratification and large during winter (Frankignoul 1985).[2]

Our scaling suggests that each of the terms in the SST equation plays a non-negligible role on decadal timescales; other dynamics may be more relevant on shorter timescales. Thus, retaining all terms and defining the air–sea flux timescale $\gamma_o = \lambda_o/C_o$ and the entrainment timescale $\gamma_e = w_e/h_{\text{mix}}$, our SST equation can be written

$$\frac{\partial}{\partial t}\text{SST}' = -\gamma_o(\text{SST}' - \theta_a') - \mathbf{u}' \cdot \boldsymbol{\nabla}\overline{\text{SST}} - \gamma_e(\text{SST}' - \theta_{\text{sub}}'). \quad (20)$$

We see that the mixed layer temperature anomaly in our model is driven toward that of the atmosphere by surface fluxes, is driven toward that of the subsurface thermal anomaly by the entrainment process, and is warmed and cooled by the advection of mean meridional SST gradient by ocean currents generated by a perturbed thermocline (see Fig. 3). The longevity of the properties of the subsurface ocean is communicated to the SST by the entrainment and advection processes, providing memory from one year to the next.

Before going on it should be mentioned that the idea of entrainment forcing of SST anomalies resembles that which is often employed in studies of equatorial coupled dynamics in which SST depends on the temperature of upwelled fluid [see Cane et al. (1990); Neelin et al. (1994)]. However, in the present context, there are some differences of interpretation. Here we interpret the relaxation term in (20) as representing the coupling of SST anomalies to deep thermal anomalies which are reexposed to the surface every winter.

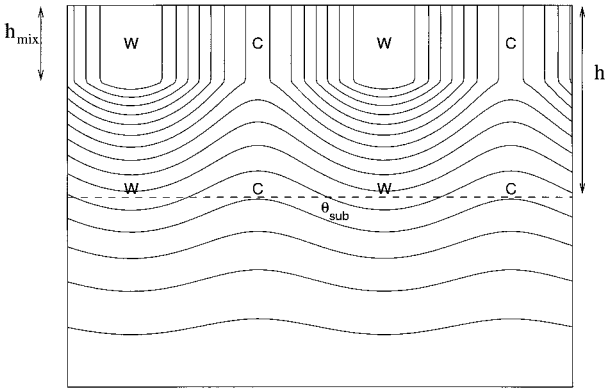


FIG. 3. Schematic diagram showing the deepening of a mixed layer into subsurface thermal anomalies associated with an undulating thermocline. Note the resulting SST anomalies.

We now assume that $\theta'_{\text{sub}}$ evolves via adiabatic undulation of isopycnal surfaces underlying the mixed layer. Where the isopycnals are perturbed upward, cold water is brought toward the surface, lowering $\theta'_{\text{sub}}$ (and thus SST) and vice versa (see Fig. 3),

$$\frac{\partial}{\partial t}\theta'_{\text{sub}} + w\frac{\partial}{\partial z}\overline{\theta_o} = 0,$$

where $w$ is the vertical velocity and $(\partial/\partial z)\overline{\theta_o}$ is a measure of the stratification of the upper ocean. Setting $w = \partial\eta/\partial t$ and integrating both sides with respect to time, the deep thermal anomaly is

$$\theta'_{\text{sub}} = -\eta\frac{\partial}{\partial z}\overline{\theta_o} = \eta\frac{N_o^2}{\varepsilon g} = \frac{1}{g\varepsilon}\frac{f}{h}\psi_o,$$

where $\eta$ is a measure of the vertical excursion of isotherms, $N_o^2 = -(g/\rho_{o0})(\partial/\partial z)\overline{\rho}$ is the Brunt–Väisälä frequency and $\varepsilon \equiv -(1/\rho_{o0})(\partial\overline{\rho}/\partial\overline{\theta})$ is the ratio of density change to temperature change. (If there are no salinity variations, $\varepsilon$ is the coefficient of thermal expansion of water.) In the above $\eta$ has been related to the baroclinic streamfunction via the thermal wind relation $\eta = (f/hN_o^2)\psi_o$.

Since $v' = (\partial/\partial x)\psi_o$ in (20) and noting that $\theta_a' = r_a\tilde{\psi}$, we can now write the evolution equation for SST in terms of the oceanic streamfunction and the atmospheric baroclinic streamfunction

$$\frac{\partial}{\partial t}\text{SST}' = -\gamma_o(\text{SST}' - r_a\tilde{\psi}) + ar_o\frac{\partial}{\partial x}\psi_o - \gamma_e(\text{SST}' - r_o\psi_o), \quad (21)$$

where

$$r_o \equiv \frac{f}{g\varepsilon h} \qquad a \equiv -\frac{1}{r_o}\frac{\partial}{\partial y}\overline{\text{SST}} = -\frac{g\varepsilon h}{f}\frac{\partial}{\partial y}\overline{\text{SST}}.$$

The parameter $r_o$ is a scaling constant between an oceanic streamfunction anomaly and the temperature as-

[2] Note that $w_e$ represents the downward velocity of the entraining base of the mixed layer through the underlying ocean: it is *not* related to the large-scale upwelling of fluid associated with the thermohaline overturning.

sociated with it via thermal wind, analogous to $r_a$, defined after (15). The parameter $a$, which is generally positive, measures the strength of horizontal advection in the SST equation: for an SST anomaly of lateral scale $L$, advection dominates over entrainment when $a/L \gg \gamma_e$.

### e. Coupled equations

Finally we may now write a set of four coupled equations for the dynamic ocean, SST, and barotropic and baroclinic atmospheric components in closed form, by inserting the forcing relations [(17), (14), and (18)] into Eqs. (16), (21), (10), and (15) to yield

dynamic ocean,

$$-\frac{1}{L_o^2}\frac{\partial}{\partial t}\psi_o + \beta\frac{\partial}{\partial x}\psi_o = \alpha\nabla^2(1/2\hat{\psi} - \tilde{\psi}); \quad (22)$$

SST,

$$\frac{\partial}{\partial t}\mathrm{SST} = -\gamma_o(\mathrm{SST} - r_a\tilde{\psi}) + ar_o\frac{\partial}{\partial x}\psi_o - \gamma_e(\mathrm{SST} - r_o\psi_o); \quad (23)$$

barotropic atmosphere,

$$\hat{U}\frac{\partial}{\partial x}\nabla^2\hat{\psi} + \hat{\beta}\frac{\partial}{\partial x}\hat{\psi} + \tilde{U}\frac{\partial}{\partial x}\nabla^2\tilde{\psi} = 0; \quad \text{and} \quad (24)$$

baroclinic atmosphere,

$$\tilde{U}\frac{\partial}{\partial x}\nabla^2\hat{\psi} + \tilde{\beta}\frac{\partial}{\partial x}\hat{\psi} + \hat{U}\frac{\partial}{\partial x}\left(\nabla^2\tilde{\psi} - \frac{2}{L_a^2}\tilde{\psi}\right) + \hat{\beta}\frac{\partial}{\partial x}\tilde{\psi} = \frac{4}{L_a^2}\gamma_a\left(\tilde{\psi} - \frac{1}{r_a}\mathrm{SST}'\right), \quad (25)$$

where $\hat{\beta}$ and $\tilde{\beta}$ are defined in Eqs. (12) and (13).

Before going on to study the properties of this coupled system it should be mentioned that the above model has some similarities with the early study of White and Barnett (1972), a paper which we found of great interest. However, they use a much simpler SST equation, and look for coupled growing modes on monthly timescales and identify waves with periods near the *barotropic* ocean Rossby wave period. Their ocean model cannot capture the slow baroclinic evolution of the ocean. Moreover the atmosphere assumed by White and Barnett neglects mean zonal winds, is linearized about a state of rest, and its thermal forcing is represented in an unusual way that is unclear to us. In the present model we shall see that the ability of the atmosphere to equilibrate to thermal forcing is vital to the presence of coupled modes, an aspect that is absent in the study of White and Barnett (1972). Our coupled system also has some aspects in common with that of Pedlosky (1975); however, Pedlosky focused on the effect of air–sea interaction on baroclinic instability, and thus retained time derivatives in the atmospheric dynamics. Finally, if the terms associated with ocean dynamics are neglected on the right side of (23), then (23)–(25) reduce to a set studied by Frankignoul (1985).

## 3. Dispersion relations and form of coupled modes

We now proceed to solve the coupled set of equations set out in section 2, show that they support coupled modes, and derive their dispersion relation. We then go on to discuss the physical mechanism behind the coupled behavior in the light of observed phenomena.

### a. Plane wave solutions

The coupled equations are linear and isotropic, and contain only even derivatives in $y$, so we look for plane wave solutions of the form

$$\hat{\psi} = \hat{\psi}'e^{i(kx-\sigma t)}\sin ly \qquad \tilde{\psi} = \tilde{\psi}'e^{i(kx-\sigma t)}\sin ly$$
$$\psi_o = \psi_o'e^{i(kx-\sigma t)}\sin ly \qquad \mathrm{SST} = \mathrm{SST}'e^{i(kx-\sigma t)}\sin ly.$$

These waves have the same spatial scale and frequency in both ocean and atmosphere; they move together in lock step, with only amplitude differences and phase offsets. Inserting these wavelike forms, canceling a common factor of $e^{i(kx+ly-\sigma t)}$ and dropping the primes for notational convenience, (22)–(25) can be written

$$\frac{i}{L_o^2}\sigma\psi_o + \beta ik\psi_o = -\alpha\kappa^2\left(\frac{1}{2}\hat{\psi} - \tilde{\psi}\right), \quad (26)$$

$$-i\sigma\mathrm{SST} = -\gamma_o(\mathrm{SST} - r_a\tilde{\psi}) + ikar_o\psi_o - \gamma_e(\mathrm{SST} - r_o\psi_o), \quad (27)$$

$$-\hat{U}ik\kappa^2\hat{\psi} + \hat{\beta}ik\hat{\psi} - \tilde{U}ik\kappa^2\tilde{\psi} = 0, \quad (28)$$

and

$$-\tilde{U}ik\kappa^2\hat{\psi} + \tilde{\beta}ik\hat{\psi} - \hat{U}ik\kappa_a^2\tilde{\psi} + \hat{\beta}ik\tilde{\psi} = \frac{4}{L_a^2}\gamma_a\left(\tilde{\psi} - \frac{1}{r_a}\mathrm{SST}\right), \quad (29)$$

where

$$\kappa^2 = k^2 + l^2$$

is the the total squared wavenumber, and

$$\kappa_a^2 = \kappa^2 + \frac{2}{L_a^2}.$$

#### 1) THE ATMOSPHERE

Because of the simplicity of our atmospheric model, we may solve Eq. (28) to find the barotropic response $\hat{\psi}$ in terms of the baroclinic flow $\tilde{\psi}$ thus

$$\hat{\psi} = -\mu\tilde{\psi}, \quad (30)$$

where

$$\mu \equiv \frac{\tilde{U}}{\hat{U} - \hat{\beta}/\kappa^2}. \tag{31}$$

The relative strength of the barotropic and baroclinic modes is controlled by $\mu$, a measure of the ratio of vertical windshear to the barotropic Rossby wave speed, Doppler-shifted by the barotropic mean wind. On scales close to that of stationary barotropic Rossby waves, $|\mu|$ is large and atmospheric perturbations are equivalent barotropic. When $|\mu|$ is small, perturbations change sign between levels 1 and 2. As described in detail in section 3a(2) the vertical structure of the atmospheric response to thermal forcing plays a key role in the coupled mode.

Turning now to the baroclinic response of the atmosphere, let us first imagine that the SST [and hence, in view of (18), $\delta\phi^*$] is fixed in space and time and consider the response of the atmosphere to a fixed SST anomaly. Equation (30) may be used to elimate $\hat{\psi}$ from (29) to yield, after dividing by $i\kappa^2$,

$$\left(\tilde{U}k\mu - \frac{\tilde{\beta}k}{\kappa^2}\mu - \hat{U}k\frac{\kappa_a^2}{\kappa^2} + \frac{\hat{\beta}k}{\kappa^2} + \frac{4i\gamma_a}{\kappa^2 L_a^2}\right)\tilde{\psi} = \frac{4i\gamma_a}{\kappa^2 L_a^2}\frac{1}{r_a}\text{SST}.$$

Let us identify the terms in the previous equation. The Newtonian relaxation process can be viewed as a balance between constant external forcing and linear damping; the terminal velocity of a falling object is a useful analog. The damping (radiative heat loss) is the imaginary term on the left, the forcing (heating from the surface) is the term on the right. The (inverse) thermal damping timescale of a PV anomaly of scale $\kappa^2$ is clearly

$$\Gamma \equiv \frac{4\gamma_a}{\kappa^2 L_a^2}. \tag{32}$$

This should be compared with an advective-propagation timescale over the same distance [stemming from the left side of (29)] given by

$$\nu \equiv -\tilde{U}k\mu + \frac{\tilde{\beta}k}{\kappa^2}\mu + \hat{U}k\frac{\kappa_a^2}{\kappa^2} - \frac{\hat{\beta}k}{\kappa^2}. \tag{33}$$

This is a measure of the frequency of free Rossby waves in the atmosphere, Doppler-shifted by the mean zonal wind. It can be interpreted as a timescale for a free atmospheric Rossby wave to travel across the heating anomaly. In terms of $\nu$ and $\Gamma$ the baroclinic response can be expressed succinctly thus

$$\left(1 + i\frac{\nu}{\Gamma}\right)\tilde{\psi} = \frac{1}{r_a}\text{SST}, \tag{34}$$

yielding information about the phase and amplitude of the atmospheric response relative to the forcing. It says that warm SST must heat the atmosphere generating atmospheric pressure anomalies which increase with height ($\tilde{\psi} > 0$) with a phase shift $<90°$. Evidently, if the thermal equilibration timescale is much faster than the advective-propagation timescale on the scale $k$ of the thermal anomaly, then $\Gamma \gg |\nu|$, so $\tilde{\psi}$ is large and is in phase with SST. Applying our formulas to Shutts' experiment (Fig. 2), the equilibrated response, plotted in Fig. 2b, has $\nu/\Gamma = 0.5$; $\mu = -3$ for the dominant wavenumber 3 response. However, if the advective-propagation timescales are short compared to the timescale of the radiative ''spring'' pulling $\theta$ back to $\theta^*$, then $|\nu| \gg \Gamma$ so the atmospheric response is weaker and out of phase with $\psi_o$. This is the ''forced'' response shown in Fig. 2a, in which $\nu/\Gamma = 2.7$; $\mu = +\frac{1}{3}$.

It is interesting to note that even though we have sought the stationary forced atmospheric response, $\tilde{\psi}$, its form is sensitive to $\nu$ because of (34) and hence to the properties of the traveling free waves of the system.

### 2) THE COUPLED MODE

We now consider the dynamic response of the ocean: SST is no longer fixed but evolves according to (27), driven by the ocean equation (26).

We may write (34) as

$$(\text{SST} - r_a\tilde{\psi}) = (\nu/\Gamma)\frac{i + \nu/\Gamma}{1 + (\nu/\Gamma)^2}\text{SST} \equiv m\text{SST}, \tag{35}$$

where $m$ is complex. Note that when the atmosphere is in the ''equilibrated mode'' ($\nu/\Gamma \to 0$), the air–sea temperature difference (and thus the surface heat flux) is zero.

Now we may use Eq. (35) to eliminate $(\text{SST} - r_a\tilde{\psi})$ from Eq. (27), solving it for SST in terms of $\psi_o$

$$\text{SST} = \left(\frac{ika + \gamma_e}{-i\sigma + \gamma_e + m\gamma_o}\right)r_o\psi_o. \tag{36}$$

Next, we eliminate SST by inserting (36) into (34)

$$\left(1 + i\frac{\nu}{\Gamma}\right)\tilde{\psi} = \left(\frac{ika + \gamma_e}{-i\sigma + \gamma_e + m\gamma_o}\right)r\psi_o, \tag{37}$$

where we have defined

$$r \equiv \frac{r_o}{r_a} = \frac{H}{2\varepsilon\theta_{a0}h}. \tag{38}$$

The scaling term $r$ sets the scale between oceanic and atmospheric streamfunction through their mutual connection to temperature.

From (37), the forcing of the atmospheric streamfunction by the oceanic streamfunction is mediated by the processes that set SST in the model. The parameter $\gamma_e$ is a measure of the strength of the entrainment process, the parameter $ak$ (which has units of 1 time$^{-1}$) is a measure of the strength of advection of SST gradients, and $m\gamma_o$ measures the influence of air–sea flux on SST. In the entrainment process, low streamfunction implies a raised thermocline, which means the mixed layer is entraining cool water, reducing SST and so cooling the atmosphere. In the advection process, meridional cur-

rents advect warm or cool SST, which also forces the atmosphere.

Equation (37) is a relation between $\tilde{\psi}$ and $\psi_o$. Another is provided by (26), which can be written, using (30)

$$(\sigma - \omega_r)\psi_o = -i\alpha\kappa^2 L_o^2\left(\frac{\mu}{2} + 1\right)\tilde{\psi}, \tag{39}$$

where $\omega_r$ is the oceanic baroclinic Rossby wave frequency

$$\omega_r \equiv -\beta k L_o^2.$$

For (39) to be consistent with (37), either $\tilde{\psi} = \tilde{\psi}_o = 0$ or

$$\left(\frac{-i\sigma + \gamma_e + m\gamma_o}{iak + \gamma_e}\right)(\sigma - \omega_r)(-\nu + i\Gamma) = r\Gamma\alpha\kappa^2 L_o^2\left(\frac{\mu}{2} + 1\right). \tag{40}$$

This is a quadratic dispersion relation for waves in our coupled system. The left side of Eq. (40) is composed of the product of three terms. The first describes the response of SST to ocean dynamics and air–sea interaction. The second describes the propagation of thermocline anomalies as Rossby waves (note the term $\omega_r$) and the third describes the quasi-stationary response of the atmosphere to SST anomalies. The right-hand side involves the feedback forcing of atmospheric windstress back onto the ocean dynamics (note the presence of $\alpha$). The solutions of Eq. (40) are

$$\sigma = \frac{1}{2}(\omega_r - i\gamma_e - i\gamma_o m) \pm i\left\{-\frac{1}{4}(\omega_r + i\gamma_e + i\gamma_o m)^2 + r(-ak + i\gamma_e)\left[\alpha\kappa^2 L_o^2\left(\frac{\mu}{2} + 1\right)\frac{\frac{\nu}{\Gamma} + i}{\left(\frac{\nu}{\Gamma}\right)^2 + 1}\right]\right\}^{1/2}. \tag{41}$$

We note immediately that the presence of imaginary terms indicates the possibility of growth or decay of the wave. The possibility of a growing coupled mode is the centerpiece of the model because infinitesimal perturbations of the system can then grow to large amplitude. If growing coupled modes exist, then they can be self-starting and sustain themselves against dissipative effects that will become more and more important as the coupled mode reaches finite amplitude.

### *b. Form and growth mechanism of coupled mode*

The complexity of (41) stems from the several different processes that play a role in the SST Equation (20). To gain an understanding of the physics of the coupling, we must simplify the dispersion relation (41). We will now consider several different cases, including only one or two terms in the SST equation, in turn, to study their influence in isolation. We will begin with the simplest case that illustrates the coupled interaction, and then consider other processes that modify this underlying mechanism.

#### 1) SST CASE 1: ENTRAINMENT

The simplest case is the one where entrainment dominates the SST equation, and advection, air–sea flux, and tendency are small. Then (20) reduces to

$$0 = -\gamma_e(\mathrm{SST} - \theta_{\mathrm{sub}})$$
$$\mathrm{SST} = \theta_{\mathrm{sub}} = r_o\psi_o, \tag{42}$$

implying perfect communication between thermocline perturbations and SST. Dominance of entrainment requires that $\gamma_e \gg ak$, $\gamma_e \gg \sigma$, $\gamma_e \gg m\gamma_o$ (numerical values are considered in section 4). Then the first term on the left side of (40) reduces to 1, and there is only one solution to the now linear equation for $\sigma$

$$\sigma = \omega_r - r\left[\alpha\kappa^2 L_o^2\left(\frac{\mu}{2} + 1\right)\frac{\frac{\nu}{\Gamma} + i}{\left(\frac{\nu}{\Gamma}\right)^2 + 1}\right]. \tag{43}$$

The waves of our system move in a phase-locked fashion through the ocean and atmosphere. Because the dynamical ocean is the only prognostic field (the SST tendency term has been neglected), from one perspective the fluctuations exist fundamentally in the ocean. They are manifest in the atmosphere because it responds to the modification of SST (and hence thermal forcing) induced by the ocean. But the ocean only moves because the atmosphere blows over it; thus our mode is a coupled one.

We see the ocean connection by the presence of the oceanic Rossby wave frequency $\omega_r$ in (43). The second term in (43) contains a real part created by air–sea in-

teraction that (slightly) slows down or speeds up the oceanic Rossby waves. But $\sigma$ also has an imaginary part:

$$\mathrm{Im}(\sigma) = -r\alpha\kappa^2 L_o^2\left(\frac{\mu}{2} + 1\right)\frac{1}{\left(\frac{\nu}{\Gamma}\right)^2 + 1}. \qquad (44)$$

Since the waves have the form $e^{i(kx-\sigma t)}\sin ly$, then $\mathrm{Im}(\sigma)$ must be positive for growth. All the variables in (44) are positive-definite except $(\mu/2 + 1)$. For $\mathrm{Im}(\sigma) > 0$, we need $\mu/2 + 1 < 0$. What is the physical meaning of this condition on $\mu$? It arose from the ''surface wind stress'' term in the oceanic forcing in (17). Since

$$\psi_s = \frac{1}{2}\hat{\psi} - \tilde{\psi} = -\left(\frac{\mu}{2} + 1\right)\tilde{\psi}$$

surface streamfunction anomalies have the same sign as the vertical shear $\tilde{\psi}$ when $\mu < -2$; that is, the waves are then equivalent barotropic.

Waves near barotropic resonance ($\hat{U} \approx \hat{\beta}/\kappa^2$, with $|\mu|$ large) exhibit the strongest barotropic response, and therefore grow the fastest. But the growth rates also depend on the size of the equilibration term $\Gamma$ relative to the advection-propagation parameter $\nu$; $\nu$ depends on $\hat{U}$, $\tilde{U}$, and the wave size. When $|\nu| \ll \Gamma$, the wave has time to equilibrate with the oceanic forcing [i.e., the left- and right-hand sides of (25) independently approach zero]. A large response will be excited, enhancing the coupling. But if advection-propagation is much more rapid than equilibration ($|\nu| \gg \Gamma$), the response of the atmosphere is smaller and shifted away from the oceanic SST anomaly, and growth of the coupled mode is slowed. These effects are encapsulated in the factor $[(\nu/\Gamma)^2 + 1]^{-1}$ in (44). It is the equilibrated atmospheric modes that couple most efficiently and grow most rapidly.

The structure of the fastest-growing mode for the entrainment-dominated SST case is sketched in Fig. 4. As described above, any mode with positive growth rate must have $\mu < -2$, so the atmospheric response is equivalent barotropic ($|\psi_1| > |\psi_2| > |\psi_s|$ and each has the same sign), weakest at the surface and strongest aloft. If the surface pressure anomaly is positive, the resultant anticyclonic surface winds will cause downward Ekman pumping in the ocean that deepens the already-deep thermocline leading [see (42)] to a warmer surface and a positive feedback. If the surface pressure anomaly is negative, Ekman dynamics will suck up the thermocline resulting in anomalously cold winter SST, again a positive feedback. For the coupling physics adopted here, coupled growth will occur whenever the atmospheric response is equivalent barotropic.

The atmospheric and oceanic wave components need not be in phase with one another, and the degree of phase-matching determines the rate at which the coupled

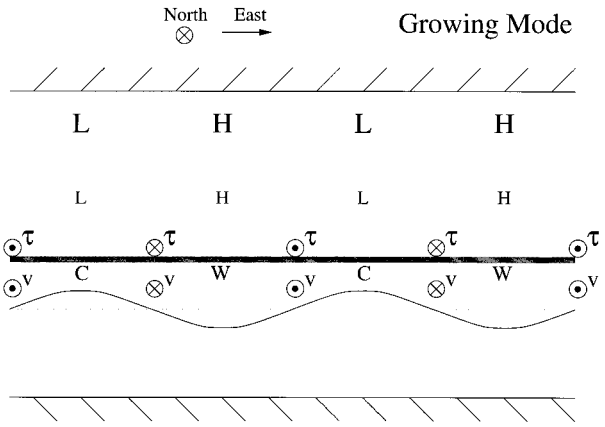


FIG. 4. Phase relationships between ocean and atmosphere for the fastest growing coupled mode. The symbols H and L denote highs and lows of atmospheric pressure, with the amplitude of the pressure anomaly increasing with height. The atmospheric response is ''equilibrated,'' as in Fig. 2b. The symbols W and C denote warm and cold SST, and the undulating line indicates the depth of the thermocline. Note the high (low) pressure above warm (cold) water, and the phase match between wind stress and current.

mode grows. Growth is fastest when $\nu/\Gamma$ is small in (44), which [from (34) and (42)] occurs when the atmosphere equilibrates completely with the underlying ocean, and high pressures occur directly over warm, deep-thermocline water ($\tilde{\psi} \propto \mathrm{SST} \propto \psi_o$). Then the Ekman pumping acts directly to increase the amplitude of thermocline perturbations; the wind applies torque to the ocean to reinforce the existing circulation. As the advection/propagation term $|\nu|$ increases, the atmospheric perturbation is ''blown away'' from the oceanic anomaly that generates it, resulting in a phase lead or lag; the Ekman pumping no longer perfectly matches the location of greatest anomaly, so growth is slower. When $|\nu|$ completely dominates $\Gamma$, the phase shift is 90° ($\tilde{\psi} \propto i\mathrm{SST}$; $\tilde{\psi} \propto \psi_o$). In this case, the Ekman pumping does not increase the thermocline anomalies at all because the wind forcing is in quadrature with the ocean response. These two cases (zero lag and quadrature) correspond to the equilibrated and directly forced modes shown in Fig. 2. More specifically, the atmospheric wave lies westward of the oceanic wave by a phase angle

$$\theta = \mathrm{Tan}^{-1}\left(\frac{\nu}{\Gamma}\right). \qquad (45)$$

If $\nu > 0$, atmospheric pressure crests lie eastward of SST maxima, and vice versa for $\nu < 0$.

For atmosphere–ocean phase shifts between 90° and −90°, in the growing mode the circulation induced by oceanic thermal forcing yields a wind stress that reinforces the sense of the preexisting circulation. If the waves are able to equilibrate with their energy source ($|\nu| \ll |\Gamma|$), growth is rapid and the atmospheric geopotential anomalies lie directly over their SST sources.

But if the waves in the atmosphere propagate away from the energy source more rapidly than that source can be renewed ($|\nu| \gg |\Gamma|$), the coupled phenomenon grows slowly, with atmospheric waves shifted downstream from their SST sources [see (34)]. In all cases of growth, though, the atmospheric anomaly hovers near the SST heat source.

It is useful to draw an analogy with a burning candle. The heat of the flame melts and vaporizes the wax directly below it, which then provides chemical energy to allow the flame to grow and maintain itself. If we blow gently on the candle flame, we may transport it away from its fuel source faster than the fuel is renewed: the flame weakens, and may die if we blow hard enough. In all cases, though, the flame hovers above or beside the wick.

#### 2) SST CASE 2: ENTRAINMENT AND TENDENCY

What happens if we include the SST tendency term in Eq. (20), but still neglect meridional advection [and therefore $ak$ in (41)]? In the limit where $ak \ll \gamma_e$, Eq. (41) reduces to

$$\sigma = \frac{1}{2}(\omega_r - i\gamma_e) \pm i\left\{-\frac{1}{4}(\omega_r - i\gamma_e)^2 - i\gamma_e\omega_r + i\gamma_e r\left[\alpha\kappa^2 L_o^2\left(\frac{\mu}{2} + 1\right)\frac{\frac{\nu}{\Gamma} + i}{\left(\frac{\nu}{\Gamma}\right)^2 + 1}\right]\right\}^{1/2}. \quad (46)$$

In the case where entrainment is much faster than Rossby propagation ($\gamma_e \gg \omega_r$) and is also faster than the air–sea coupling ($\gamma_e \gg r[\ ]$), we may use the approximation $\sqrt{1 + x} \approx 1 + x/2$ to find the approximate solutions

$$\sigma_1 \approx \omega_r - r\alpha\kappa^2 L_o^2\left(\frac{\mu}{2} + 1\right)\frac{\frac{\nu}{\Gamma} + i}{\left(\frac{\nu}{\Gamma}\right)^2 + 1} \quad (47)$$

and

$$\sigma_2 \approx -i\gamma_e + r\alpha\kappa^2 L_o^2\left(\frac{\mu}{2} + 1\right)\frac{\frac{\nu}{\Gamma} + i}{\left(\frac{\nu}{\Gamma}\right)^2 + 1}. \quad (48)$$

The first solution is identical to the entrainment solution without the tendency term (43), described in detail in section 3b(1). The second solution is dominated by rapid SST damping through entrainment (i.e., by the $-i\gamma_e$ term). The Rossby wave propagation term canceled in the expression for $\sigma_2$, the solution does not propagate as a Rossby wave and is, in fact, decoupled from the dynamic ocean; therefore we call it an ''SST-only'' mode. The second term, describing the air–sea interaction, has the opposite sign in the SST-only mode as in the ''entrainment mode'' discussed in section 3b(1) suggesting that the conditions for growth discussed there cause enhanced decay in this mode.

The structure of the SST-only mode is quite simple, and is depicted in Fig. 5. We begin with a warm patch of SST, but with only a slightly perturbed thermocline having the opposite sign as SST. The SST patch generates an atmospheric response above or downstream from it (depending on $\nu/\Gamma$), but the patch is rapidly damped by the $\gamma_e$ (SST $-$ $\theta_{\text{sub}}$) term in (20), and decays in a short time $1/\gamma_e$. The slight Ekman pumping supplied by the wind during that time acts only to diminish the initial thermocline anomaly; thus all fields decay to zero rapidly.

The two solutions span the range of possible initial conditions for SST and $\psi_o$. If we begin with an arbitrary pattern of SST and $\psi_o$, the component that has SST and $\psi_o$ in phase will grow and propagate as described in section 32(a) (assuming conditions for growth are met), while the out-of-phase component will decay rapidly via the process described here, until only the in-phase component is observed.

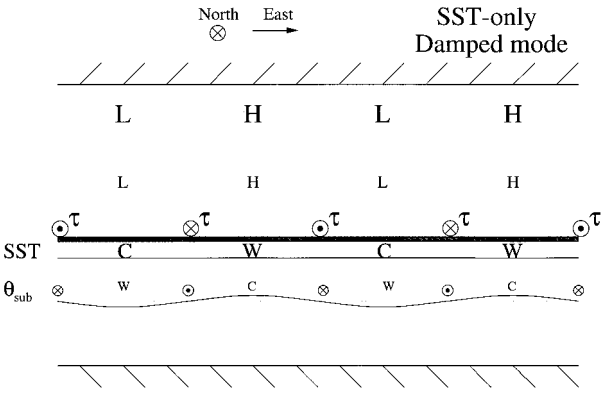


FIG. 5. Configuration of the rapidly damped SST-only mode (48). SST is out of phase with the very small subsurface thermal anomalies, leading to rapid damping of SST.

### 3) SST CASE 3: ADVECTION AND TENDENCY

Even though our SST scaling analysis suggests that entrainment is at least as important as advection in winter months, it is useful to consider the advection mechanism in isolation. Accordingly, we consider the form of the SST (20) with $\gamma_e \to 0$ and $\gamma_o \to 0$,

$$\frac{\partial}{\partial t}\mathrm{SST}' = -\mathbf{u}' \cdot \nabla\overline{\mathrm{SST}}.$$

In the same limit, the dispersion relation (41) becomes

$$\sigma = \frac{1}{2}\omega_r \pm i\left\{-\frac{1}{4}\omega_r^2 - rak\left[\alpha\kappa^2 L_o^2\left(\frac{\mu}{2}+1\right)\frac{\frac{\nu}{\Gamma}+i}{\left(\frac{\nu}{\Gamma}\right)^2+1}\right]\right\}^{1/2}. \tag{49}$$

As before, we consider the case where the coupling term $rak[\ ]$ is smaller than the Rossby wave propagation term $\omega_r$, in which case we get the following two approximate solutions:

$$\sigma_1 = \omega_r - \frac{rak}{\omega_r}\left[\alpha\kappa^2 L_o^2\left(\frac{\mu}{2}+1\right)\frac{\frac{\nu}{\Gamma}+i}{\left(\frac{\nu}{\Gamma}\right)^2+1}\right] \tag{50}$$

and

$$\sigma_2 = \frac{rak}{\omega_r}\left[\alpha\kappa^2 L_o^2\left(\frac{\mu}{2}+1\right)\frac{\frac{\nu}{\Gamma}+i}{\left(\frac{\nu}{\Gamma}\right)^2+1}\right]. \tag{51}$$

The solution $\sigma_1$ has exactly the same structure as the entrainment mode described in section 3b.1 with $r$ replaced by $rak/\omega_r$. Growth occurs in this ''advection mode'' when the atmosphere responds with barotropic highs over warm water, exactly as in section 3b(1).

Like the entrainment mode, the advection mode has warm SST where $\psi_o$ is large (see Fig. 4), but for an entirely different reason, illustrated in Fig. 6. Oceanic streamfunction anomalies will propagate from east to west. A streamfunction high (depressed thermocline) will generate a northward flow to its west, advecting warm water from the south and creating a warming trend there. When the $\psi_o$ anomaly propagates to that spot, the advection ceases, and so does the warming. When the $\psi_o$ anomaly continues on to the west, it generates southward flow, bringing cold water that cools the SST patch. Therefore, a maximum in SST is observed at the maximum in $\psi_o$, and appears to follow that maximum as it propagates westward. SST and $\psi_o$ are in phase, and waves which propagate more slowly have more time to build up larger SST anomalies: this is why the Rossby wave propagation term occurs in the denominator of the second term in $\sigma_1$.

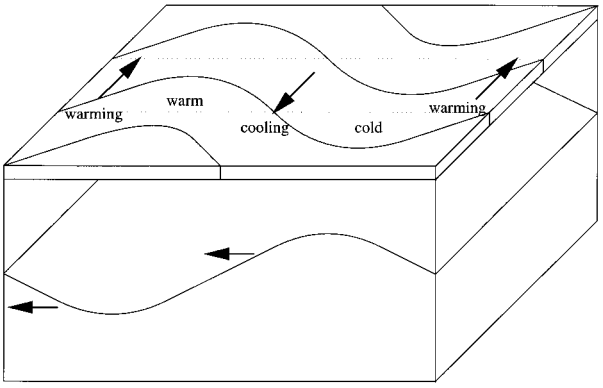


FIG. 6. The process by which advection of mean meridional SST gradient leads to warm SST anomalies over deep-thermocline water.

The second solution has no Rossby wave propagation, and SST and $\psi_o$ are out of phase. The solution is most strongly damped when air–sea coupling is strong.

### 4) SST CASE 4: AIR-SEA FLUX, ENTRAINMENT, AND TENDENCY

The inclusion of the surface flux term into the SST equation should reduce the growth of the coupled mode. After all, if a warm patch of SST is losing heat to the atmosphere at a rate comparable to the rate of heating by entrainment or advection, the anomaly will have smaller magnitude and thus generate a less powerful atmospheric circulation. However, the most rapidly growing mode from the previous three cases is unaffected by the air–sea flux term. Our fastest-growing mode has $\nu/\Gamma = 0$, so $m = 0$ in (35) and SST $= \theta_a = r_a\tilde{\psi}$. There is no air–sea temperature difference (complete equilibration), so the surface heat flux shuts off. In fact, by setting $m = 0$ in (40), we get (46) when advection is small.

We now consider the case where $m$ is nonzero, but for convenience we assume advection is small ($ak \ll \gamma_e$); our results will also hold for non-negligble $ak$. In the limit $m\gamma_o \gg \omega_r$ and $m\gamma_o \gg r[\ ]$, Eq. (41) can be approximated by

$$\sigma_1 \approx \omega_r - \frac{\gamma_e}{\gamma_e + m\gamma_o} r\alpha\kappa^2 L_o^2\left(\frac{\mu}{2}+1\right)\frac{\frac{\nu}{\Gamma}+i}{\left(\frac{\nu}{\Gamma}\right)^2+1} \tag{52}$$

and

$$\sigma_2 \approx -i\gamma_e - i\gamma_o m + \frac{\gamma_e}{\gamma_e + m\gamma_o} r\alpha\kappa^2 L_o^2\left(\frac{\mu}{2}+1\right)\frac{\frac{\nu}{\Gamma}+i}{\left(\frac{\nu}{\Gamma}\right)^2+1}. \tag{53}$$

These two modes closely resemble the entrainment modes discussed in section 3b(2); however, the coupled growth term of the coupled solution ($\sigma_1$) is multiplied by the factor $\gamma_e/(\gamma_e + m\gamma_o)$, and damping of the SST-only solution ($\sigma_2$) is enhanced by air–sea flux. If $\gamma_e \approx \gamma_o$ (typical of the annual average), growth off-resonance (where $\|m\| \sim 1$) is reduced by about a factor of 2. During the winter, when $\gamma_e$ is larger than $\gamma_o$, growth will not be significantly affected. During the summer, when $\gamma_e \sim 0$, Eqs. (52) and (53) reduce to

$$\sigma_1 \approx \omega_r \qquad \sigma_2 \approx -i\gamma_o m = \frac{\nu/\Gamma - i(\nu/\Gamma)^2}{1 + (\nu/\Gamma)^2}\gamma_o. \quad (54)$$

Coupling between the geostrophic ocean and the mixed layer has ceased entirely; the first solution takes the form of uncoupled propagating oceanic Rossby waves with no expression in the mixed layer or atmosphere; the second equation shows the effect of a two-layer quasigeostrophic (QG) atmosphere over a ''swamp'' mixed layer. This mode resembles the ''QG atmosphere over a copper plate'' discussed by Frankignoul (1985). It is characterized by rapidly damped patterns in SST and atmosphere that propagate eastward or westward depending on the phase of the atmosphere's response to SST. If warm SST produces warm air to the east of the SST anomaly ($\nu/\Gamma > 0$), this warmth results in a heat flux back into the ocean farther east than it originated, resulting in eastward phase propagation, and vice versa for westward phase shifts. However, since this ''heat flux'' mode is always damped on a timescale of order $\gamma_o^{-1} \sim 8$ months, it is unlikely to play a role in decadal variability.

Allowing air–sea flux to affect the mixed layer cannot destroy our growing mode, because the fastest-growing mode has vanishingly small air–sea flux. However, it may reduce growth rates somewhat when conditions are slightly off-resonance. When air–sea flux dominates over entrainment (as might happen in summer), the mixed layer decouples from the dynamic ocean; Rossby waves continue to propagate in the thermocline while the mixed layer exhibits rapidly damped air–sea interaction as described by Frankignoul (1985).

## 4. Discussion of solutions: Predictions and sensitivity

We now discuss the numerical values of the various parameters that characterize our model and go on to consider its relevance to middle-latitude air–sea coupling. Comparisons of our model with observed variability patterns are also made.

### *a. Frequency and scales*

Oceanic Rossby waves with a frequency of $\omega_r = 2 \times 10^{-8}$ s$^{-1}$ have a wave period of 10 yr or so and thus could be implicated in decadal variability. This then implies a zonal wavenumber of $k = \pi\,(5500\text{ km})^{-1}$ (for $L_o = 45$ km and $\beta = 1.8 \times 10^{-11}$ s$^{-1}$ m$^{-1}$), a scale comparable to that of an ocean basin, and commensurate with, for example, the scales of the leading modes of variability found by Deser and Blackmon (1993) and Cayan (1992). It turns out that the modification of the real part of the phase speed associated with coupling [the second term in (43)] is comparatively small (see below) and does not make a significant difference to the phase speed. Our advection and entrainment coupled modes propagate at essentially the speed of internal oceanic Rossby waves.

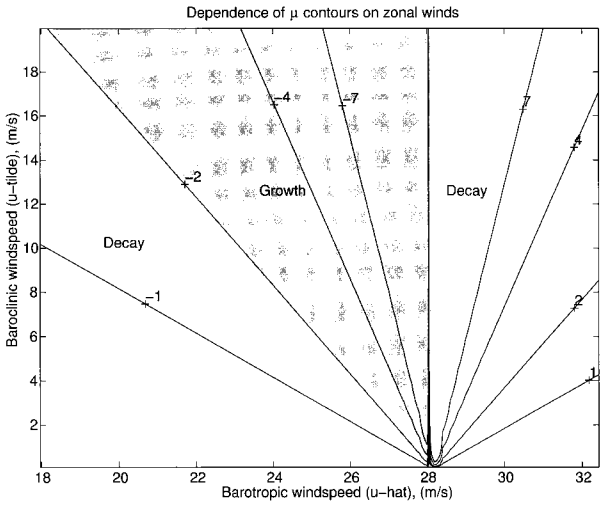


FIG. 7. Contours of $\mu$ from (31) as a function of barotropic ($\hat{U} = u_1 + u_2$) and baroclinic ($\tilde{U} = u_1 - u_2$) wind speed, for a particular choice of wavenumber [$k = \pi/(5500$ km), $l = \pi/(3200$ km)]. A growing coupled mode is possible when $\mu < -2$ (the shaded region of the figure).

In Fig. 7, $\mu$ is plotted as a function of $\hat{U}$ and $\tilde{U}$ for a wave of size comparable to the NAO; $k = \pi$ (5500 km)$^{-1}$ and $l = \pi$ (3200 km)$^{-1}$. For $\hat{U} > \hat{\beta}/\kappa^2 = 28$ m s$^{-1}$, $\mu$ is positive, implying an atmospheric response that switches sign between upper and lower levels, leading to a decaying mode. In the lower-left part of the figure, $0 > \mu > -2$, again implying damping. An equivalent barotropic response (and therefore a growing mode) will occur if the zonal winds fall in the central triangular region. This can readily be achieved by typical middle-latitude tropospheric winds.

### *b. Coupling constants*

#### 1) MECHANICAL

Let $\alpha'$ scale the stress of the wind, $\tau$, to the surface wind speed $u_s$ thus

$$\tau' = \alpha' u_s'. \quad (55)$$

To deduce a value for $\alpha'$, consider the bulk aerodynamic drag law for the total (mean + anomaly) wind stress (see Gill 1982),

$$\overline{\tau} + \tau' = c_D \rho_a (\overline{u_s} + u_s')^2,$$

where $c_D$ is the drag coefficient. After linearizing about the mean $\overline{u_s}$, we obtain

$$\tau' = 2c_D\rho_a\overline{u_s}u_s' \tag{56}$$

allowing us to identify

$$\alpha' = 2c_D\rho_a\overline{u_s}.$$

Comparing (17), (55), and (56), we see that

$$\alpha = \frac{\alpha'}{\rho_{o0}h} = \frac{2c_D\rho_a\overline{u_s}}{\rho_{o0}h}.$$

In accord with observations, for $\overline{u_s} = 5$ m s$^{-1}$, $h = 500$ m, we find that $\alpha \approx (2 \times 1.3 \times 10^{-3} \times 1 \times 5)/(10^3 \times 500) = 3 \times 10^{-8}$ s$^{-1}$ = (1.1 yr)$^{-1}$ if $c_D = 1.3 \times 10^{-3}$.

#### 2) THERMAL EQUILIBRATION

The inverse damping timescale of a PV anomaly, $\Gamma \equiv (4\gamma_a)/(\kappa^2 L_a^2)$, Eq. (32), depends on the scale of the anomaly relative to the deformation radius and the radiative-convective restoring timescale. Inserting typical numbers we find

$$\Gamma \equiv \left[4\frac{1}{14 \text{ day}}\left(\frac{10^3 \text{ km}}{660 \text{ km}}\right)^2\right]$$
$$= 7.7 \times 10^{-6} \text{ s}^{-1} = \frac{1}{1.5 \text{ day}}.$$

This timescale becomes shorter the greater the scale of the anomaly relative to the deformation radius.

#### 3) SST

By putting numbers into (38) we find that the SST coupling parameter $r \equiv H/(2\varepsilon\theta_{a0}h) \approx 10^4$ $(2 \times 10^{-4} \times 290 \times 500)^{-1} \approx 340$. A reasonable value for $a$ is $a \equiv (gh\varepsilon/f)(\partial/\partial y)\overline{\text{SST}} = 10 \times 500 \times 10^{-4}/10^{-4}$ $3 \times 10^{-6} = 0.015$ m s$^{-1}$. With $k = 5 \times 10^{-7}$ m$^{-1}$, the advection timescale is $ak = 7.5 \times 10^{-9}$ s$^{-1}$. In section 2d(2), we established the entrainment parameter $\gamma_e = 1.3 \times 10^{-7}$ s$^{-1}$ and the air–sea flux parameter $\gamma_o = 5 \times 10^{-8}$ s$^{-1}$. If $\sigma \sim \omega_r \sim 2 \times 10^{-8}$ s$^{-1}$, then for this choice of parameters $\gamma_e \gg \sigma$, $\gamma_e \gg ak$, $\gamma_e > \gamma_o$, so the entrainment solution should dominate in the full dispersion relation (40), perhaps with some contribution from air–sea flux. Furthermore, the second and third terms beneath the radical in (41) are smaller than the first, so the approximation leading to (47) and (48) should be valid. We now compute growth rates as a function of wavelength and other parameters to see if this is indeed the case.

### c. Growth rates

In Fig. 8, growth rate is plotted as a function of zonal wavelength, using the values for mean winds and coupling constants given in Table 1. These parameters are for a ''winter'' simulation, in which the entrainment term is large. In Figs. 8a and 8b, we show the two solutions to (41), which include all terms in the SST equation. Figures 8c and d show the two solutions to (46), which include SST entrainment and tendency, along with their approximate solutions (that is, (47) = (43) and (48)). Figures 8e and 8f show the two solutions for the advection-only mode (49) along with their approximations (50) and (51).

We observe a highly scale-selective growing mode with an *e*-folding time of 1–2 yr. Only those wavelengths that allow nearly stationary free waves to exist (i.e., $\nu \approx 0$) produce the phase matching between atmosphere and ocean and the equivalent barotropic atmospheric response necessary for the coupled growing mode. Even though the entrainment timescale $(\gamma_e)^{-1}$ is only 2.5 times faster than the air–sea interaction timescale $(\gamma_o)^{-1}$, the solution including only entrainment and tendency (solid line in Fig. 8c) or even entrainment alone (dashed line in Fig. 8c) provides a good approximation to the growth rate of the full SST equation. This latter approximation is based on the incredibly simple entrainment-dominated SST equation SST $= r_o\psi_o$ [section 3b(1)].

Note that, as expected from section 3b(3), the advection-tendency SST equation exhibits growth under the same conditions as the entrainment SST equation. The entrainment mode and the advection mode are completely compatible and noninterfering, and are, in fact, nearly indistinguishable in their SST, dynamic ocean, and atmospheric patterns.

For both entrainment and advection solutions, growth is most rapid for high (low) pressure anomalies above warm (cold) water, in accordance with observations of the correlation between SST and surface pressure anomalies seen in the observations and models on interannual-to-decadal timescales (see Deser and Blackmon 1992; Latif and Barnett 1996).

The growth rate and phase speed of the SST-only mode dominated by surface heat flux [$\sigma_2$ in (54)] is shown in Fig. 9. The wave propagation direction changes from eastward to westward as we cross over the wavelength of stationary free atmospheric waves, and the damping reduces to zero (because $m = 0$ when $\nu/\Gamma = 0$). We can explain the reduced damping at resonance of the SST-only mode of the full SST equation (Fig. 8b) by noting that both entrainment and air–sea flux tend to damp SST when the system is off-resonance, but the air–sea flux shuts off at resonance.

We see, then, that both the entrainment and the advection process generate coupled growing modes with similar growth rates and nearly identical wavelength dependence and structure (i.e., Fig. 4 applies to both). The largest term in the SST equation (the entrainment process) appears to dominate the behavior of the coupled mode for the parameters chosen here, but if we decrease $\gamma_e$ (as might happen when summer begins) advection begins to dominate the growing mode. In Fig. 10, we show the dispersion relation when $\gamma_e = 0$. The

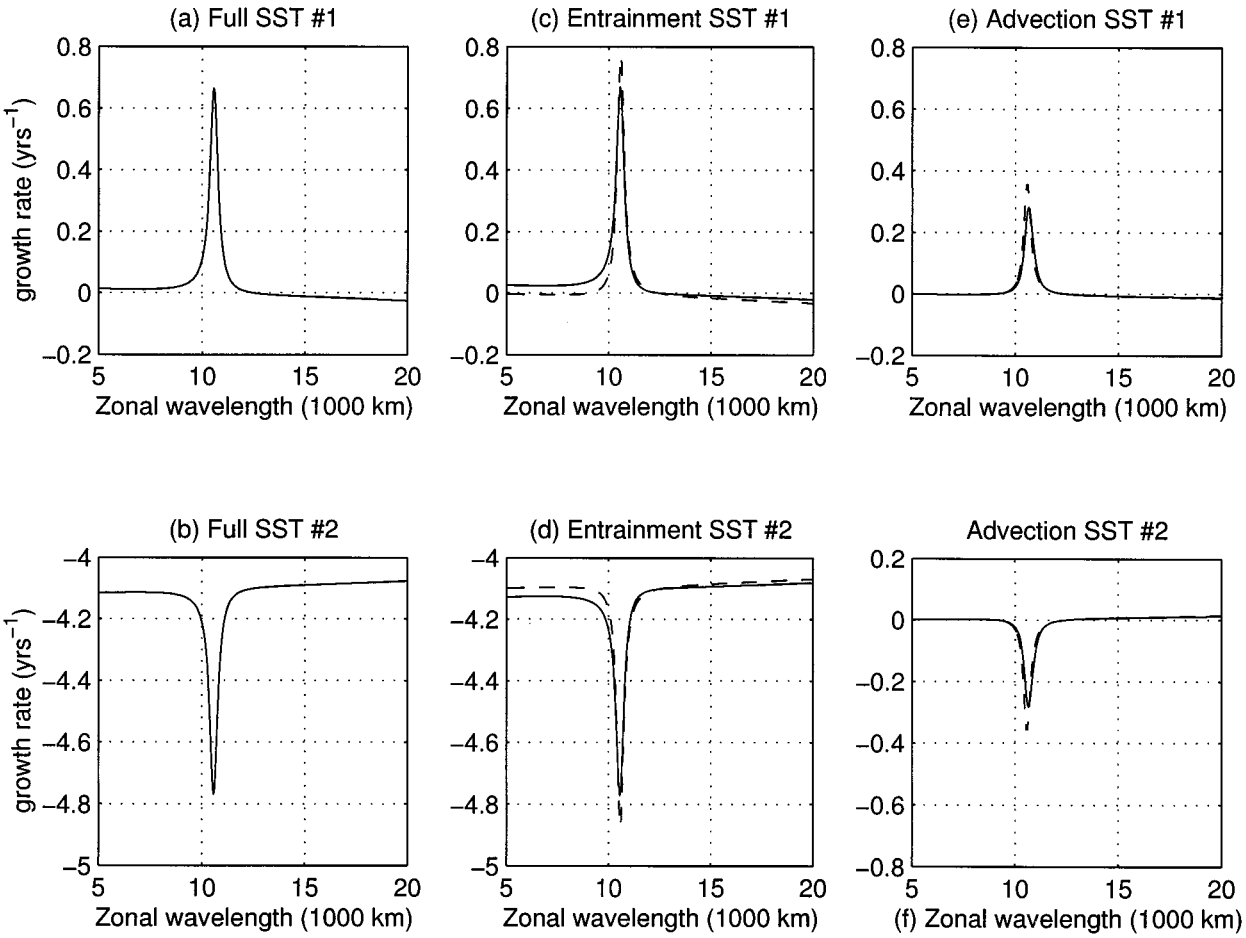


FIG. 8. Graph of growth rate [Im($\sigma$)] as a function of wavenumber for the coupled dispersion relation (41) and its simplified forms. (a) and (b) The two solutions to (41) given the parameters in Table 1. Solid lines in (c) and (d) For (46), which neglects SST advection and air–sea flux; dashed lines are for the simplified forms (47) and (48). (e) and (f) For (49), which neglects entrainment; dashed lines are for the simplified forms (50) and (51).

TABLE 1. Numeric parameter values.

| Quantity | Variable | Value |
|---|---|---|
| Coriolis parameter | $f$ | $1 \times 10^{-4}$ s$^{-1}$ |
| Beta | $\beta$ | $1.8 \times 10^{-11}$ (m s)$^{-1}$ |
| Meridional wavenumber | $l$ | $\pi$ (3200 km)$^{-1}$ |
| Atmospheric scale height | $H$ | 10 km |
| Ocean upper-layer thickness | $h$ | 500 m |
| Mixed layer thickness | $h_{\text{mix}}$ | 100 m |
| Oceanic Rossby radius | $L_o$ | 45 km |
| Atmospheric Rossby radius | $L_a$ | 660 km |
| Wind stress coupling constant | $\alpha$ | $3 \times 10^{-8}$ s$^{-1}$ |
| Ocean density–temperature | | |
| Scale factor | $\varepsilon$ | $10^{-4}$ K$^{-1}$ |
| SST advection parameter | $\alpha$ | 0.015 m s$^{-1}$ |
| Atmospheric air–sea flux parameter | $\gamma_a$ | $8 \times 10^{-7}$ s$^{-1}$ = (14 day)$^{-1}$ |
| Oceanic air–sea flux parameter | $\gamma_o$ | $5 \times 10^{-8}$ s$^{-1}$ = (8 month)$^{-1}$ |
| Mixed layer entrainment parameter | $\gamma_e$ | $1.3 \times 10^{-7}$ s$^{-1}$ = (3 month)$^{-1}$ |

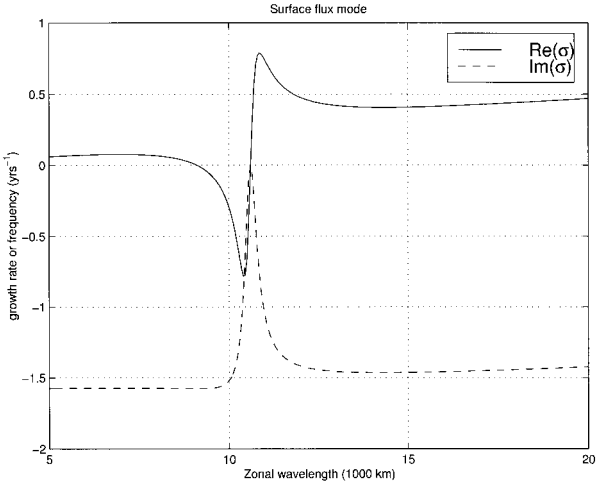


FIG. 9. Real and imaginary parts of frequency for the heat flux mode discussed in section 3b(4). Note change in propagation direction and cessation of damping at resonance.

air–sea flux term does not affect the fastest-growing mode (again, because $m = 0$ there), but it does reduce off-peak growth rates, narrowing the peak width. There is a region of weak damping for wavelengths shorter than the wavelength of maximum growth. When air–sea flux is large, the phase shift between wind stress and subsurface streamfunction can be greater than 90°, so the wind torque opposes the subsurface vorticity. However, note that "wintertime" growth at this wavelength (Fig. 8) outweighs the damping, and the solutions for an annual-average value of $\gamma_e$ ($7 \times 10^{-8}$ s$^{-1}$; not shown) show no damping region.

As one might expect, growth rates also depend on the strength of the mean zonal winds. Figure 11 shows contours of the growth rate of the entrainment-only solution (44) for $k = \pi$ (5500 km)$^{-1}$ basin-scale modes (other parameters are as in Table 1) as a function of baroclinic and barotropic winds. The growth rates range from years to decades for a broad range of atmospheric winds. Growth only occurs in the shaded triangle, where $\mu < -2$ (see Fig. 7). The winds needed to fall in the growth region are consistent with those over the midlatitude oceans.

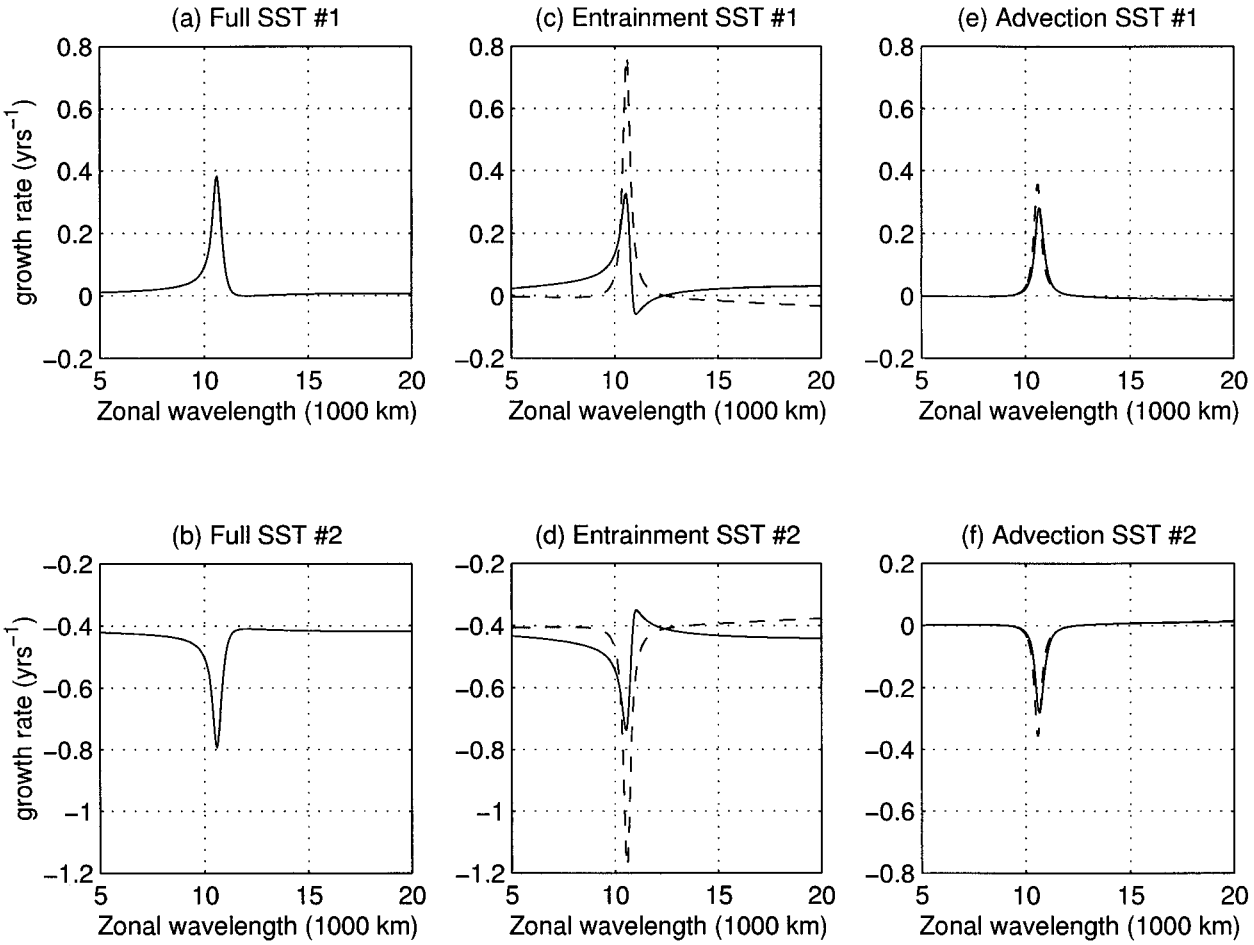


FIG. 10. As in Figs. 8a,b, but with zero entrainment: $\gamma_e = 0$.

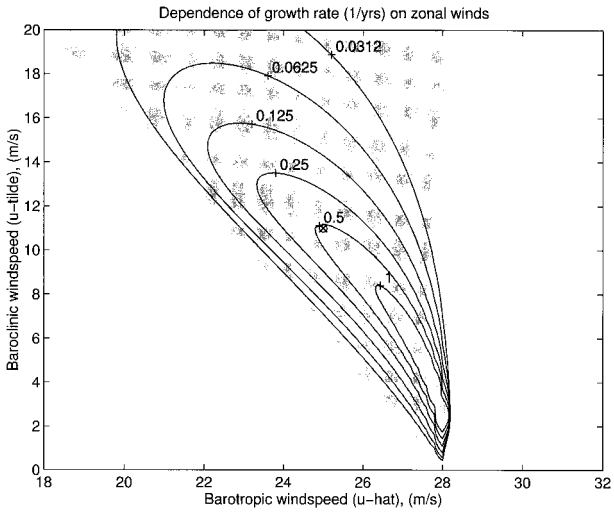


FIG. 11. Contours of growth rate [Im($\sigma$)] from (43) in yr$^{-1}$ as a function of baroclinic ($\hat{U} = u_1 - u_2$) and barotropic ($\hat{U} = u_1 + u_2$) zonal mean wind speed for a particular choice of wavenumber [$k = \pi$/(5500 km), $l = \pi$/(3200 km)]. The zonal winds used to produce Fig. 11 are marked here with a $\otimes$.

From these figures, we see that atmosphere–ocean anomalies the size of the midlatitude North Pacific or North Atlantic (commensurate with the scales of the NAO and Pacific–North American pattern) can exhibit fluctuations of decadal period and exponential growth in our model for reasonable choice of basic state. The growth and surface expressions of these modes appear strongest in the winter, when entrainment tightly couples SST with the thermocline's structure. The model predicts equivalent barotropic atmospheric highs over warm SST, similar to that seen in observations of decadal variability (e.g., Kushnir 1994).

The largest growth rate of the coupled mode is quite rapid, with an *e*-folding timescale of 1.3 yr. This is almost certainly fast enough to maintain the wave against dissipative processes that have not been modeled here. One might feel that growth is, in fact, *too* rapid. After all, this model suggests an increase in amplitude of $e^5 \sim 150$ in a single Rossby wave period. However, numerous unmodeled processes will conspire to limit the growth. For example, the real coupled system certainly has important dissipative processes unmodeled here. The real ocean has time-mean currents that will try to rip the coherent Rossby waves apart before they reach large amplitude. The presence of meridional walls will limit the lifetime and therefore growth of an individual Rossby wave. Finally, in nature there are strong seasonal changes; the terms composing the SST equation vary strongly with season, as does the zonal wind pattern. The seasonal cycle is unlikely to affect the existence and propagation of the thermocline perturbations that form the ''memory'' of our system (since the cessation of entrainment in the summer tends to decouple the thermocline from the mixed layer), but the mode might only be expressed in the SST and atmosphere during the wintertime, restricting the growth to six months out of the year.

In addition to inducing growth, the coupled physics also modifies the phase speed of oceanic Rossby waves through the real part of the coupling term [see (41)]. When the atmospheric response is slightly westward, the wind stress accelerates the waves toward the west, and vice versa for an eastward atmospheric response. This wave frequency shift measures only 20% of the Rossby wave speed for the parameters chosen here. Note, however, that the phase speed of the fastest-growing mode is not affected at all.

### *d. Comparison with the Antarctic Circumpolar Wave*

The Antarctic Ocean circles the globe without continents and is periodic in the zonal direction. Here the progress of oceanic Rossby waves are less impeded by meridional boundaries than in the gyre regimes of ocean basins, so perhaps the unbounded model described above is more directly applicable here than elsewhere. Let us see whether the present model can support coupled oscillations in the Antarctic Ocean.

Our previous discussions show that conditions for growth depend crucially on the sign of $r$ and $a$. However, these quantities remain positive definite in the Southern Hemisphere despite changes in the sign of $f$ and $(\partial/\partial y)\overline{\mathrm{SST}}$. All the results of section 3 still apply. According to our model, growth of decadal-scale coupled waves could occur in the Southern Ocean if the atmospheric response to SST forcing is equivalent barotropic and if highs are located above warm water.

Recently, White and Peterson (1996) and Jacobs and Mitchell (1996) described an ''Antarctic Circumpolar Wave'' (ACW), which takes the form of a wavenumber-2 perturbation of SST, surface air pressure, sea surface height, wind stress, and sea ice extent, circling eastward around Antarctica with a period of around 4 yr. Jacobs and Mitchell report that sea surface height (a proxy for oceanic streamfunction $\psi_o$) is coincident with SST. Both White and Peterson and Jacobs and Mitchell report that wind stress curl (and hence, to the extent that the geostrophic approximation is appropriate at the surface, surface air pressure anomaly) appears to lead SST by 90° phase in the observations. This configuration is summarized in Fig. 12.

By using parameters appropriate to the Antarctic Ocean [$U_1 = 15$ m s$^{-1}$, $U_2 = 5$ m s$^{-1}$, $l = \pi$ (3100 km)$^{-1}$, $\beta = 1.6 \times 10^{-11}$(m s)$^{-1}$, other parameters as in Table 1], we obtain a growing mode of wavenumber 2 around the globe, a growth rate of 0.35 yr$^{-1}$, and a westward phase speed of 4 cm s$^{-1}$. Our model assumes an ocean at rest; to adapt it to the Antarctic Ocean, we simply suppose our model dynamics occur in a frame moving eastward with the Antarctic Circumpolar Current at 10–15 cm s$^{-1}$. The resultant phase speed ''over

ground'' for our waves is 5–10 cm $s^{-1}$ eastward. SST, $\psi_o$, and $\hat{\psi}$ are all approximately in phase.

This wave has some similarity to the ACW, but also some important differences. Phase speed and wavelength are in good agreement, as is the phase match between SST and $\psi_o$. However, our model predicts that the surface air pressure (and therefore wind stress curl) should be in phase with SST. Observations of the ACW show a 90° phase shift.

Our model can produce phase-shifted growing modes in two ways. An off-resonant wave would have a significant phase shift (since $\nu/\Gamma \neq 0$) between atmosphere and ocean; such an off-resonant wave might be demanded by periodicity constraints. Furthermore, the tendency term in the SST (20) can allow the SST response to lag behind the forcing produced by the dynamic ocean. Moreover the requirement that the amplitude of SST grow over time means some phase-shifting must occur to allow the dynamic ocean to supply additional warmth to regions where SST is already large.

The model can support growing modes with phase shifts, but it is difficult to generate phase shifts much larger than 45°. In addition, we note that if the atmosphere–ocean phase shift is truly 90°, we must have $\nu/\Gamma \to \infty$ [see (45)], which means that the atmospheric response to SST anomalies [see Eq. (34)] is zero, and growth does not occur [see (44)]. While this could be an artifact of the atmospheric model chosen, we note that a 90° lag between wind stress curl and $\psi_o$ implies that the wind stress cannot increase the amplitude of the oceanic streamfunction. The wind stress is zero when the currents are maximum and vice versa, so no work is done on the current, again making growth impossible. We conclude that either the phase relationships in nature are not as the presently available observations suggest, or the Antarctic Circumpolar Wave does not grow through wind stress feedback coupling.

While preparing this paper for submission, we became aware of a study by Qiu and Jin (1997) that applies a model similar to ours to the ACW. Their SST equation resembles that of section 3b(3), but allows cooling of SST anomalies by air–sea flux. They employ a greatly simplified atmosphere that ignores $\beta$-effects and Rossby waves (essentially a thermodynamic equation plus thermal wind), in which the response is assumed a priori to be equivalent barotropic. Their ocean dynamics and coupling assumptions are similar to ours, but with two oceanic levels and a mean zonal current. A coupled growing mode and a damped uncoupled mode are found, just as in this study. However, our use of a more dynamically based, albeit still highly simplified, description of the atmosphere leads to differences that cannot be ignored. The meridional wavelength and zonal windspeeds chosen by Qiu and Jin are so small that any reasonable choice of the baroclinic component of the mean winds (a factor not part of their model) generates a baroclinic response in our model, with $\mu > 0$ [see (31)]. This leads to a decaying mode in our equations. Their assumption that the atmosphere responds barotropically agrees with observations of the ACW, but it is not trivial to explain or generate such a response through atmospheric dynamics. Most importantly, however, our model and that of Qiu and Jin adopt the same mechanical forcing of the ocean by wind stress, and so theirs, like ours, must prohibit growth when wind stress curl leads oceanic streamfunction by 90°.

The model described here, that of Qiu and Jin, and the observations have their limitations. We note that Christoph and Barnett (1996) have observed an ACW in their ECHAM4 + OPYC3 coupled numerical model. Because the model may provide a continuous record of all relevant fields over many decades (particularly wind and surface air pressure fields, which are difficult to measure remotely) it may be fruitful to test our analytical model against this numerically simulated ACW.

### *e. Sensitivity to parameters*

The parameters of our model are rather schematic and grossly represent a myriad of processes. However, in the entrainment-tendency and advection-tendency limits, $\alpha$, $r$, $\gamma_e$, and $a$, which are perhaps the most uncertain of the external parameters, appear only as multipliers to the coupled growth terms in (47) = (43) and (50), approximations to (41). As such, changing their values causes a proportional change in the growth rate of the coupled wave, but not its structure or existence. Likewise, $\Gamma$ changes only the width of the peaks in figure 8, which is relatively unimportant. Larger $\Gamma$ implies more rapid equilibration, allowing a wider range of atmospheric waves to be in the equilibrated state.

The structure and existence of a growing coupled mode depends on $\mu$ and $\nu$, and therefore on $U_1$, $U_2$, $\beta$, $k$, and $l$. Experimentation has shown that most reasonable midlatitude values of $U_1$, $U_2$, $l$, and $\beta$ result in growth at some zonal wavelength $k$; however, the wavelength of the fastest-growing mode is rather sensitive to the choice of these variables. By changing the zonal winds or meridional wavenumber by 20%, can change the wavelength of maximum growth in Fig. 8 by 50% or more. Frankignoul (1985) also noticed the ease in which a two-layer QG model can be ''tuned'' using the meridional wavenumber. Growing coupled modes are thus a robust feature of this model, but their precise sizes and shapes are not. This is to be expected of a simple model intended to illustrate a process rather than to simulate reality.

### *f. Energetics of growth mechanism*

Where does the energy for growth come from? While our model does not rigorously conserve energy, we may still consider the energetics of the natural system with true mechanical and thermal energy fluxes in both air and sea, closing the energy budget. The atmosphere gains energy from the ocean through surface heat flux

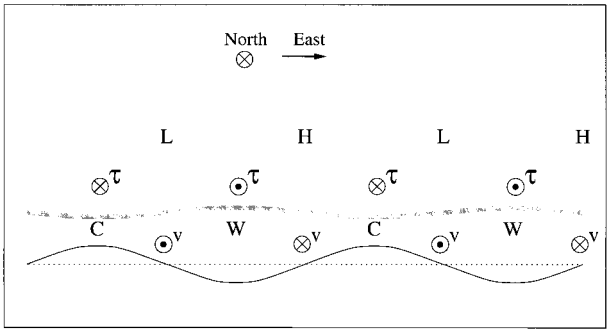


FIG. 12. Schematic summary of the ACW based on observed correlations between SST (W = warm, C = cold), atmospheric sea level pressure (H = high, L = low), meridional wind stress ($\tau$), and sea surface height observed by White and Peterson and Jacobs and Mitchell. The wave encircles Antarctica with wavenumber 2, and travels eastward at 10 cm $s^{-1}$.

and loses energy through surface wind stress drag. The storage of energy in the atmosphere is small, so these two processes approximately balance. The ocean therefore ''sees'' the atmosphere as a device that converts thermal energy (from surface heat flux) into mechanical energy (via wind stress).

Consider the entrainment-dominated SST parametrization of section 3b(1). If the interface between two ocean layers with temperature difference $\Delta T$ is anomalously low by an amount $\Delta h$, that column of water has an extra amount of heat (thermal energy) per unit area of magnitude,

$$E_{\text{th}} = C_p \rho \Delta h \Delta T.$$

This heat is tied to an SST anomaly and so is accessible to the atmosphere through air–sea interaction. If a nearby column has the opposite perturbation $-\Delta h$, the atmosphere can be thought of as a heat engine which removes heat from the warm patch and supplies it to the cold patch, diverting some of that heat flux to do ''useful work'' (i.e., generate a wind stress). This wind stress can increase the kinetic ($E_k$) and gravitational potential energy ($E_p$) of the ocean. Since our anomalies are much larger than the oceanic Rossby radius, $E_p \gg E_k$ (Gill 1982). The gravitational potential energy density of the above configuration, that is, the amount of energy per unit area that must be imparted by the wind to lift an interface between fluids of density difference $\Delta\rho$ a height $\Delta h$, is

$$E_p = \frac{g}{2}\Delta\rho(\Delta h)^2 = \frac{g}{2}\varepsilon\rho\Delta T(\Delta h)^2,$$

where $\varepsilon = \Delta\rho/\rho\Delta T$, equivalent to the coefficient of thermal expansion if salinity is constant. The thermal energy contained in this anomaly is much, much greater than the energy required to make it available,

$$\frac{E_{\text{th}}}{E_p} = \frac{C_p}{(g/2)\varepsilon\Delta h} \approx 1.6 \times 10^5,$$

for $\Delta h = 50$ m, $C_p = 4000$ J $kg^{-1}$ $K^{-1}$, and $\varepsilon = 10^{-4}$ $K^{-1}$. So if the atmospheric heat engine is just 0.0006% efficient at converting the lateral thermal energy difference into wind stress which further lifts the interface, the coupled wave can replenish its energy store.

We thus see that the energy for growth comes from the huge amount of thermal energy stored in the thermocline, which is usually unavailable to the ocean dynamics. But the application of wind stress tilts the thermocline, turning vertical thermal gradients into horizontal gradients that the atmosphere can use in a heat-engine fashion to create a wind stress that further tilts the thermocline. The atmosphere is a ''catalyst,'' allowing the ocean to extract energy from the vertical stratification. An identical argument holds for the meridional-advection SST equation: the energy for growth is now extracted from the mean meridional SST gradient.

## 5. Conclusions

We have described and analysed a simple atmosphere–ocean model that supports growing coupled modes and exhibits decadal oscillations in SST, air pressure, and oceanic streamfunction. Moreover, the growth rate and form of the coupled modes have aspects in common with observations of natural variability in the North Atlantic, the North Pacific, and the Antarctic Circumpolar Wave. The ''clock'' of the coupled model is provided by oceanic baroclinic Rossby waves [in this manner, it resembles the model of Latif and Barnett (1994)]. Undulations of the subsurface thermal field, associated with the westward-propagating baroclinic Rossby waves, exposed to the surface by wintertime mixed layer deepening, induce SST anomalies that change the diabatic heating rates of the atmosphere and hence its circulation. The resulting anomalous winds blow over the ocean and exert a stress on it; in the growing mode, this anomalous wind stress acts to amplify subsurface undulations, leading to larger deep thermal anomalies and magnified SST anomalies, resulting in a positive feedback.

We find that the vertical structure of the atmospheric response to thermal forcing is central to the coupling mechanism. In order to support a growing mode the response must be equivalent barotropic, with highs above warm water. If the Doppler-shifted atmospheric Rossby wave speed is sufficiently slow, so that the time it takes to cross an SST anomaly is long compared to the thermal equilibration timescale, ($|\nu|/\Gamma \ll 1$), then thermal equilibration will occur and coupled modes grow rapidly enough to maintain themselves against dissipative processes.

Two approaches to the specification of SST were considered. In the first, SST was tied to subsurface thermal anomalies associated with vertical undulations in isotherms. In the second SST was determined by horizontal circulation across a specified large-scale meridional SST gradient. Both ''recipes'' yield growing modes with

very similar structure. The former model exhibits more rapid growth for the parameters chosen in this study, and (at least for the parameters chosen here) the limit where entrainment completely dominates SST provides an excellent, simpler approximation to the full dispersion relation. Air–sea heat flux, the third important influence on SST, acts to reduce the growth rate, but does not affect the fastest-growing mode at all, because that mode has negligible air–sea temperature difference. The coupling mechanism is most active during periods of rapid entrainment (winter); the mode may become less strongly coupled and therefore ''dormant'' during the summer, though subsurface Rossby waves will continue to propagate during dormancy.

Comparisons of such a simple model with observations must be rather tentative. There is evidence that the response of the atmophere to SST anomalies on internnual timescales is equivalent barotropic with highs over warm surface anomalies [see, e.g., Kushnir (1994)]. Moreover, we find that the structure and growth rate of the fastest growing coupled mode is broadly consistent with what is known of the spatial scale, and low-frequency variability of the NAO. Our mode will be much more strongly coupled in the winter, in agreement with Hurrell and van Loon's (1997) and others' observation that the NAO is strongest and shows greatest persistence in winter. There are also some aspects that resemble the ACW, although observed air–sea phase relationships appear to differ from this model's predictions.

However, in relating this simple model to phenomema in the atmosphere and ocean, one must proceed with care. The coupling parameters $\alpha$ and $r$ are poorly known, the true barotropic and baroclinic modes of the atmosphere are complicated pressure-weighted averages of vertical quantities rather than the simple two-level sum and difference used here, and quasigeostrophy and the $\beta$-plane approximation give only qualitative guidance on such large scales, particularly near resonance. Any of the these factors could significantly change the numerical values of $\mu$, $\nu$, and $\Gamma$.

Our use of a two-level QG atmosphere can easily be criticized. In nature the response of the atmosphere is sensitive to the upper-boundary conditions (a rigid lid was assumed here, which may overemphasize the downstream stationary wave response by prohibiting upward transmission of wave energy) and the vertical profile of heating (which is trivial in a two-layer model). Our model may also be suspect near resonance, as other dynamics may become important.

Of even more importance, perhaps, are the lack of zonal asymmetries in our model. The model ocean has no meridional boundaries (there are *no* landmasses) and the mean flow of the atmosphere is not purely zonal. However, nearly stationary atmospheric waves also exist in nonuniform flows. For example, Marshall and Molteni (1993) seek ''neutral vectors'' of the free atmosphere, and find free, almost-stationary waves that can coexist with climatological winds. Moreover they strongly resemble EOF's of the low-frequency variability and have an uncanny resemblance to observed low-fequency variability patterns like the NAO. In the real atmosphere, these neutral vectors may take the place of the linear nearly stationary Rossby waves that can efficiently couple with the ocean in this model.

We christen this growth mechanism a ''candle instability'' by analogy with a burning candle. The candle's flame feeds on the energy in the molten wax while melting more wax, ensuring a constant fuel supply, in the same way that our atmospheric model feeds on the SST anomalies, while driving a circulation which replenishes those anomalies. The candle flame and our growing mode's atmosphere also react similarly to strong atmospheric advection.

*Acknowledgments.* This work was supported by NSF Grant OSP-63568 and the NOAA Office of Global Programs.

## REFERENCES

Barnett, T. P., 1985: Variations in near-global sea level pressure. *J. Atmos. Sci.,* **42,** 478–501.

Barsugli, J. J., and D. S. Battisti, 1998: The basic effects of atmosphere–ocean thermal coupling on midlatitude variability. *J. Atmos. Sci.,* **55,** 477–493.

Battisti, D. S., U. S. Bhatt, and M. A. Alexander, 1995: A modeling study of the interannual variability in the wintertime North Atlantic Ocean. *J. Climate,* **8,** 3067–3083.

Cane, M. A., M. Munnich, and S. E. Zebiak, 1990: A study of self-excited oscillations of the tropical ocean–atmosphere system. Part I: Linear analysis. *J. Atmos. Sci.,* **47,** 1562–1577.

Cayan, D., 1992a: Latent and sensible heat flux anomalies over the northern oceans: The connection to monthly atmospheric circulation. *J. Climate,* **5,** 354–369.

——, 1992b: Latent and sensible heat flux anomalies over the northern oceans: Driving the sea surface temperature. *J. Phys. Oceanogr.,* **22,** 1743–1753.

Charney, J. G., and A. Eliassen, 1949: A numerical method for predicting the perturbations of middle latitude westerlies. *Tellus,* **1,** 38–54.

Curry, R. G., and M. S. McCartney, 1997: Labrador sea water carries northern climate signal south. *Oceanus,* **39** (2), 24–28.

Deser, C., and M. Blackmon, 1993: Surface climate variations over the North Atlantic Ocean during winter: 1900–1989. *J. Climate,* **6,** 1743–1753.

Dickson, R., J. Lazier, J. Meincke, and P. Rhines, 1996: Long-term coordinated changes in the convective activity of the North Atlantic. *Decadal Climate Variability: Dynamics and Predictability,* NATO ASI Series I: Global Environmental Change, D. L. T. Anderson and J. Wilebrand, Eds., Vol. 44, Springer, 211–261.

Frankignoul, C., 1985: Sea surface temperature anomalies, planetary waves, and air–sea feedback in the middle latitudes. *Rev. Geophys.,* **23** (4), 357–390.

——, and K. Hasselman, 1977: Stochastic climate models. Part II: Application to sea surface temperature variability and thermocline variability. *Tellus,* **29,** 284–305.

——, P. Muller, and E. Zorita, 1997: A simple model of the decadal response of the ocean to stochastic wind forcing. *J. Phys. Oceanogr.,* **27,** 1533–1546.

——, A. Czaja, and B. L'Heveder, 1998: Air–sea feedback in the North Atlantic and surface boundary conditions for ocean models. *J. Climate,* **11,** 2310–2324.

Gill, A., 1982: *Atmosphere–Ocean Dynamics.* Academic Press, 662 pp.

Griffies, S. M., and E. Tziperman, 1995: A linear thermohaline oscillator driven by stochastic atmospheric forcing. *J. Climate,* **8,** 2440–2453.

Hall, N., and S. Manabe, 1997: Can local linear stochastic theory explain sea surface temperature and salinity variability? *Climate Dyn.,* **13,** 167–180.

Hasselmann, K., 1976: Stochastic climate models. Part I: Theory. *Tellus,* **28,** 473–485.

Hurrell, J. W., 1995: Decadal trends in the North Atlantic oscillation: Regional temperatures and precipitation. *Science,* **269,** 676–679.

——, and H. van Loon, 1997: Decadal variations in climate associated with the North Atlantic oscillation. *Climate Change,* **36,** 301–326.

Jacobs, G. A., and J. L. Mitchell, 1996: Ocean circulation variations associated with the Antarctic Circumpolar Wave. *Geophys. Res. Lett.,* **23,** 2947–2950.

James, I. N., and P. M. James, 1989: Ultra-low frequency variability in a simple atmospheric model. *Nature,* **342,** 53–55.

Kushnir, Y., 1994: Interdecadal variations in North Atlantic sea surface temperature and associated atmospheric conditions. *J. Climate,* **7,** 141–157.

Latif, M., and T. P. Barnett, 1994: Causes of decadal climate variability over the North Pacific and North America. *Science,* **266,** 634–637.

——, and ——, 1996: Decadal climate variability over the North Pacific and North America: Dynamics and predictability. *J. Climate,* **9,** 2407–2423.

——, A. Grötzner, M. Münnich, E. Maier-Reimer, S. Venzke, and T. P. Barnett, 1996: A mechanism for decadal climate variability. *Decadal Climate Variability: Dynamics and Variability,* NATO ASI Series I: Global Environmental Change, D. L. T. Anderson and J. Wilebrand, Eds., Vol. 44, Springer, 263–292.

Lorenz, E. N., 1975: *Climate Predictability: The Physical Basis of Climate Modeling.* GARP Publ. Ser., Vol. 16, World Meteorological Organization.

Marshall, J., and D. K. So, 1990: Thermal equilibration of planetary waves. *J. Atmos. Sci.,* **47,** 963–978.

——, and F. Molteni, 1993: Toward a dynamical understanding of planetary-scale flow regimes. *J. Atmos. Sci.,* **50,** 1792–1818.

McCartney, M. S., R. G. Curry, and H. F. Bezdek, 1997: North Atlantic's transformation pipeline chills and redistributes subtropical water. *Oceanus,* **39** (2), 19–23.

Neelin, J. D., M. Latif, and F.-F. Jin, 1994: Dynamics of coupled ocean–atmosphere models: The tropical problem. *Annu. Rev. Fluid Mech.,* **26,** 617–659.

Palmer, T. N., 1996: Predictability of the atmosphere and oceans: From days to decades. *Decadal Climate Variability: Dynamics and Predictability,* NATO ASI Series I: Global Environmental Change, D. L. T. Anderson and J. Wilebrand, Eds., Vol. 44, Springer, 83–155.

Pedlosky, J., 1975: The development of thermal anomalies in a coupled ocean–atmospheric model. *J. Atmos. Sci.,* **32,** 1501–1514.

——, 1987: *Geophysical Fluid Dynamics.* Springer-Verlag, 710 pp.

Qiu, B., and F.-F. Jin, 1997: Antarctic circumpolar waves: An indication of ocean–atmosphere coupling in the extratropics. *Geophys. Res. Lett.,* **24,** 2585–2588.

Saravanan, R., and J. C. McWilliams, 1997: Stochasticity and spatial resonance in interdecadal climate fluctuations. *J. Climate,* **10,** 2299–2320.

——, and ——, 1998: Advective ocean–atmosphere interaction: An analytical stochastic model with implications for decadal variability. *J. Climate,* **11,** 165–188.

Shutts, G., 1987: Some comments on the concept of thermal forcing. *Quart. J. Roy. Meteor. Soc.,* **113,** 1387–1394.

Smagorinsky, J., 1953: The dynamical influence of large-scale heat sources and sinks on the quasi-stationary mean motion of the atmosphere. *Quart. J. Roy. Meteor. Soc.,* **79,** 342–366.

Sutton, R. T., and M. R. Allen, 1997: Decadal predictability of North Atlantic sea surface temperature and climate. *Nature,* **338,** 563–566.

Weng, W., and J. D. Neelin, 1998: On the role of ocean–atmosphere interaction in midlatitude interdecadal variability. *Geophys. Res. Lett.,* **25,** 167–170.

White, W. B., and T. P. Barnett, 1972: A servomechanism in the ocean/atmosphere system of the midlatitude North Pacific. *J. Phys. Oceanogr.,* **2,** 372–381.

——, and R. G. Peterson, 1996: An Antarctic circumpolar wave in surface pressure, wind, temperature and sea-ice extent. *Nature,* **380,** 699–702.